INVESTIGATION OF MICROBUBBLES AND NANOBUBBLES GAS FLOTATION FOR OIL SEPARATION FROM MARINE OILY WASTEWATER USING RESPONSE SURFACE METHODOLOGY

by

Wanhua Shen

B.Sc., Wenzhou University, 2019

THESIS SUBMITTED IN PARTIAL FULFILLMENT OF
THE REQUIREMENTS FOR THE DEGREE OF
MASTER OF SCIENCE
IN
NATURAL RESOURCES AND ENVIRONMENTAL STUDIES

UNIVERSITY OF NORTHERN BRITISH COLUMBIA

December 2022

Abstract

Oily wastewater caused by marine oil spills brings great harm to the environment. In this work, the application of gas flotation with microbubbles and nanobubbles in separating crude oil droplets from oily wastewater is reported. The experiments were conducted in a flotation column with an internal diameter of 5.2 cm and a height of 100 cm. Response surface methodology was employed to examine the effects of three experimental factors (initial oil concentration, flotation time, and temperature of inlet wastewater) on the oil separation performance and the interaction between experimental factors. A good agreement was obtained between the predicted and experimental data of oil separation efficiency, with a high R^2 of 0.99 and an adjusted R^2 of 0.98. The optimization results demonstrate that the maximum oil separation efficiency (98.3%) was achieved under optimum experimental conditions of 524.5 mg/L initial oil concentration, 28.6 min flotation time, and 21.2°C inlet wastewater temperature.

List of Publications

This master thesis yielded one published manuscript for Chapter 2, while the other chapters are combined into one paper and ready for submission. There is another paper (not included in the thesis) which is already published based on this master's research. Publication and authorships of the papers were listed as follows (Published or prepared for submission):

Shen, W., Mukherjee, D., Koirala, N., Hu, G., Lee, K., Zhao, M., & Li, J. (2022). Microbubble and nanobubble-based gas flotation for oily wastewater treatment: A review. Environmental Reviews, (ja). (Chapter 2)

Shen, W., Koirala, N., Mukherjee, D., Lee, K., Zhao, M., & Li, J. (2022). Tween 20 Stabilized Conventional Heavy Crude Oil-In-Water Emulsions Formed by Mechanical Homogenization. Frontiers in Environmental Science, 486.

Shen, W., Mao, J., Hu, G., Zhao, M., & Li, J. (2022). Investigation of microbubbles and nanobubbles gas flotation for oil separation from oily wastewater using response surface methodology. (Prepared for submission)

Table of Contents

Abstract ii
List of Publications iii
Table of Contents iv
List of Tables vii
List of Figures viii
Glossary x
Acknowledgement xii
Chapter 1 Introduction 1
Chapter 2 Literature Review* 4
2.1 Introduction 4
2.2 Properties of MBs and NBs 7
2.2.1 Bubble size 7
2.2.1.1 Size definition 7
2.2.1.2 Size measurement 8
2.2.1.3 Bubble size impact factor 9
2.2.2 Specific surface area 11
2.2.3 Zeta potential 12
2.2.4 Rising velocity 14
2.2.5 Internal pressure 15
2.2.6 Stability of NBs 16
2.3 Generation of MBs and NBs 19
2.3.1 Pressurized dissolution type 19
2.3.2 Venturi type 20
2.3.3 Swirl flow type 22
2.3.4 Porous membrane type 23
2.3.5 Ultrasonic irridation type 23
2.3.6 Electrolysis type 24
2.4 Gas flotation 26
2.4.1 Dissolved gas flotation 30
2.4.2 Induced gas flotation 33
2.4.3 Electrolytic flotation 34

2.5 Design parameters for gas flotation 36
2.5.1 Gas dissolution 36
2.5.2 Gas holdup 37
2.5.3 Recycle ratio 38
2.5.4 Interfacial tension 38
2.5.5 Spreading coefficient 39
2.6 Factors affecting oil separation efficiency in gas flotation 40
2.6.1 Initial oil concentration 40
2.6.2 pH 41
2.6.3 Temperature 42
2.6.4 Pressure 43
2.6.5 Salinity 44
2.6.6 Flotation time 45
2.6.7 Oil droplet size 46
2.7 Discussion and conclusions 47
Chapter 3 Materials and Methods 49
3.1 Materials 49
3.2 Oil weathering 50
3.3 Preparation of oily wastewater 50
3.4 Experimental setup and procedure 51
3.5 Experimental design 52
3.6 Microscopy analysis 55
3.7 Oil concentration analysis 56
Chapter 4 Results and Discussion 57
4.1 Size distribution of NBs 57
4.2 Regression model generation and statistical analysis 57
4.3 Effect of process parameters on oil separation efficiency 60
4.3.1 Effect of initial oil concentration 60
4.3.2 Effect of flotation time 63
4.3.3 Effect of temperature of inlet wastewater 64
4.3.4 Interaction of parameters 65
4.4 Response surface optimization and validation of optimized results 67
4.5 Control experiments 68
4.6 Effect of crude oil condition on oil separation efficiency 69

Chapter 5 Conclusions 71
5.1 Research summary 71
5.2 Limitations and future research 72
References 74

List of Tables

Chapter 2

Table 2.1 Different factors affecting bubble size 10

Table 2.2 Different factors affecting zeta potential 13

Table 2.3 The change of NB concentration and mean diameter in a specific period of time 18

Table 2.4 Comparison of different bubble generation methods 25

Table 2.5 Application of gas flotation system for treating oily wastewater 27

Table 2.6 Summary of different types of gas flotation systems 29

Table 2.7 Summary of different gases used in DGF system for wastewater treatment 32

Table 2.8 List of oil droplet size measurement methods 47

Chapter 3

Table 3.1 Physiochemical properties of fresh and weathered CHCO 49

Table 3.2 Summary of bubble generator specifications 51

Table 3.3 Experimental range and levels of independent variables 54

Table 3.4 Experimental matrix of CCD design with oil separation results 54

Chapter 4

Table 4. 1 Results for oil separation efficiency of CHCO 57

Table 4.2 ANOVA results of the regression model for oil separation efficiency 58

Table 4.3 Validation results with the actual and the predicted efficiency 67

List of Figures

Chapter 2

Figure 2.1 Summarized diameter range of MBs and NBs 8

Figure 2.2 Photo of MBs and NBs from a phase-contrast microscope (provided by K. Takahashi, personal communication, 2022) 9

Figure 2.3 Contaminant separation efficiency with and without NBs 12

Figure 2.4 Schematic diagram showing the behavior of MBs and NBs under water (modified from Agarwal et al. 2011) 16

Figure 2.5 Bubble generation methods 19

Figure 2.6 Pressurized dissolution type bubble generator (modified from Arumugam, 2015) 20

Figure 2.7 Venturi type bubbe generator (modified from Zhao et al., 2017; Li et al., 2017) 21

Figure 2.8 Swirl liquid flow type bubble generator (modified from Parmar and Majumder, 2013) 22

Figure 2.9 Schematic of DGF system (modified from Behin and Bahrami, 2012) 30

Figure 2.10 Different flow schemes of DGF system, (a) full-flow pressurization, (b) split-flow pressurization, and (c) recycled flow pressurization (modified from Radzi 2016) 32

Figure 2.11 Schematic of IGF system (modified from Zasadowski et al., 2014) 33

Figure 2.12 Schematic of EF system (modified from Palaniandy et al., 2017) 35

Figure 2.13 Schematic diagram of two different contact modes between oil droplet and gaseous bubbles (modified from Zhang et al., 2016) 40

Figure 2.14 The effect of pH on oil separation efficiency using MBs gas flotation 42

Figure 2.15 The effect of flotation time on oil separation efficiency 46

Chapter 3

Figure 3.1 Cumulative mass loss of CHCO at different times 50

Figure 3.2 Laboratory MBs and NBs flotation setup (a) and appearance of MBs in test water (b) 52

Chapter 4

Figure 4.1 Particle size distribution of NBs..... 57

Figure 4.2 Predicted effects of experimental factors on oil separation efficiency, (a) flotation time: 20 min, temperature of inlet wastewater: 21 °C; (b) initial oil concentration: 400 mg/L, temperature of inlet wastewater: 21 °C; (c) initial oil concentration: 400 mg/L, flotation time: 20 min 62

Figure 4.3 Effect of flotation time on oil separation efficiency..... 64

Figure 4.4 3D response surface graph showing the interaction effects of experimental factors on oil separation efficiency at (a) temperature of inlet wastewater = 21°C; (b) initial oil concentration = 400 mg/L; (c) flotation time = 20 min 66

Figure 4.5 Comparison of oil separation efficiency between gravity separation and gas flotation 68

Figure 4.6 Microscopic images and corresponding oil droplet size distribution plots of the generated oily wastewater (a) with fresh CHCO, (b) with weathered CHCO..... 69

Figure 4.7 Effect of CHCO condition on oil separation efficiency 70

Glossary

ANOVA	Analysis of variance
CHCO	Conventional heavy crude oil
CCD	Central composite design
DAF	Dissolved air flotation
DGF	Dissolved gas flotation
DI	Deionized
DLS	Dynamic Light Scattering
EF	Electrolytic flotation
GHG	Greenhouse gases
IAF	Induced air flotation
IFT	Interfacial tension
IGF	Induced gas flotation
LD	Laser diffraction
MPRI	Multi-Partner Oil Spill Research Initiative
MBs	Microbubbles
NBs	Nanobubbles
NTA	Nanoparticle tracking analysis
PVC	Polyvinyl chloride
RSM	Response surface methodology
R^2	Coefficient of determination
SDS	Sodium dodecyl sulfate
USEPA	United States Environmental Protection Agency

UPW	Ultrapure water
ZP	Zeta potential
WCSB	Western Canada Sedimentary Basin

Acknowledgement

This thesis reflects the final part of my master's study at the University of Northern British Columbia. First of all, I am deeply grateful to my supervisor, Dr. Jianbing Li, for his insightful thoughts, valuable suggestions, encouragement and support throughout my research and study. He gave me great opportunities to work on different projects and present my research in conferences, which helped strengthen my research skills and improve my confidence.

I would like to express my sincere gratitude to Dr. Min Zhao and Dr. Ronald W. Thring for serving as my co-supervisor and supervisory committee member. I greatly appreciate their quick response, insightful comments, and great discussions. My gratitude also goes to Dr. Guangji Hu, who served as a postdoctoral fellow in our research group, for his valuable feedback on my papers. I would also like to thank Conan Ma for his help with lab materials supply and sample delivery at Chemstore.

Moreover, I would like to extend my sincere thanks to people in my research group for their kind help and valuable discussions; they are Dixuan Li, Cheng Lu, Narayan Koirala, Ashkan Hosseinipooya, and Nahid Hassanshahi. I would also like to thank all my lovely friends that I have met in Canada and all my friends back in China for always being thoughtful and supportive.

Finally, I would like to dedicate this work to my family for their unconditional love and support. Without their understanding and encouragement in the past three years, it would be impossible for me to complete my master's degree. Specially thanks go to my mother, who takes care of all the family members and works hard to provide a better life for the family. She is the one who has taught me to thrive through hard times. And my father, who has showed me to embrace the beauty of life and stay positive no matter what, for which I will always be thankful.

Chapter 1 Introduction

Large amounts of oily wastewater are generated from various activities, including oil and gas production (Pendashteh et al., 2012), metal manufacturing (An et al., 2017), food processing (Zhao et al., 2021), petroleum refining processes (Hoseini et al., 2015), and marine oil spill response (Liang and Esmaeili, 2021). Offshore oil spills have been of significant concern due to their negative and long-term environmental impacts (Li et al., 2016c). When an oil spill occurs in the ocean, it undergoes various chemical, physical, and biological processes such as spreading, evaporation, dissolution, photo-oxidation, and biodegradation which collectively turn the fresh oil into weathered oil (Liu et al., 2012; Bacosa et al., 2021). The process of weathering extends the lifespan of oil in the marine environment, making its negative impacts more persistent and harmful (Mishra and Kumar, 2015). When oil is spilled on the marine water surface, with the presence of wind, waves, and currents in the ocean, adequate agitation is created on the spilled oil that leads to mixing with the underlying water and reaches the shorelines, causing damage to both aquatic and terrestrial ecosystems (Chen et al., 2021).

Different technologies have been developed to separate oil from oily wastewater, including centrifugation (Issaka et al., 2015), ultrafiltration (Kumar et al., 2017), bioremediation (Sun et al., 2019), microwave irradiation (Lemos et al., 2010), and chemical demulsification (Kang et al., 2018). These technologies have different advantages and limitations. For example, centrifugation and microwave irradiation are associated with high energy consumption (Yau et al., 2017). On the other hand, membrane fouling can lead to an increased cost of ultrafiltration, and the periodic cleaning of the membrane is necessary (Shi et al., 2014). The screening of effective chemicals for separating different types of oil is time-consuming (Kang et al., 2018). Also, the use of chemicals is hazardous to human health and the environment (Esmaeili et al., 2021). Although

bioremediation is considered environmentally friendly and sustainable, it is a very slow treatment process and is sensitive to environmental conditions (Zolfaghari et al., 2016). Therefore, there is a great need to explore other oily wastewater treatment technologies that are effective, environmentally friendly, and scalable.

Flotation has been extensively used in the separation of oils from polluted water due to its high separation efficiency and throughput, low operational cost, less sludge production, and easy operation (da Silva et al., 2015; Cai et al., 2017; Rocha e Silva et al., 2018). It is a physical separation process based on the attachment of oil droplets to gas bubbles to increase the buoyant force of oil droplets by forming oil-bubble agglomerates, which significantly accelerates oil floating to the surface of the water (Saththasivam et al., 2016; Chakibi et al., 2018). Several studies have been conducted to investigate oily wastewater treatment using gas flotation technology. For example, Tansel and Pascual (2011) used dissolved air flotation (DAF) to treat fuel oil-contaminated pond water with an initial oil concentration of 1500 mg/L, and they achieved 87% petroleum hydrocarbon separation after 30 min of batch operation. Eftekhardadkhah et al. (2015) conducted laboratory-scale induced gas flotation (IGF) experiments to separate three types of crude oil emulsions, and they observed the highest oil separation efficiency for the heaviest crude oil, which reached 98% separation after 10 min of flotation. Rajak et al. (2015) investigated the application of air flotation to the separation of emulsified light crude oil and observed higher separation efficiency at higher salinity and longer flotation time. However, so far limited studies have been reported on the application of microbubbles (MBs) and nanobubbles (NBs) gas flotation technology for marine oil spill response operation. In addition, the in-depth effects of influential factors have not been well studied. Thus, a comprehensive study of the application of MBs and NBs gas flotation to oily wastewater is necessary.

In this study, the separation of conventional heavy crude oil (CHCO) droplets in saline water with gas flotation by MBs and NBs is examined. Three experimental factors, including initial oil concentration, flotation time, and temperature of inlet wastewater, are investigated on the oil separation efficiency using response surface methodology (RSM). The main objective of this study was to evaluate the effects of different parameters on oil separation efficiency and the interactions between the considered variables, as well as to find optimum treatment conditions and to predict the oil separation efficiency within the investigated parameter range. The results would provide valuable information on the development of reliable and effective technology to separate oil from oily wastewater in a sustainable manner and lay a solid foundation for scaling up this technology for field application.

Chapter 2 Literature Review*

*This review has been published as: Shen, W., Mukherjee, D., Koirala, N., Hu, G., Lee, K., Zhao, M., & Li, J. (2022). Microbubble and nanobubble-based gas flotation for oily wastewater treatment: A review. Environmental Reviews, (ja).

2.1 Introduction

Oily wastewater is generated from oil spill incidents and many other sources, such as food processing, oil refining, textile and leather industries, metal rolling and finishing, paper deinking, and petrochemical industries (Hassan et al., 2015; Huang et al., 2018). Different types of oil and oil components can be found in wastewater, such as animal grease, crude oil, lubricating oil, and cutting oil, depending on the source of wastewater generation (Putatunda et al., 2019). Marine oil spills are regarded as a major threat to the environment. The growing maritime transportation of petroleum products has led to increased risks of oil spills from ships and other oil handling facilities (Transports Canada, 2017). Once an oil spill has occurred, proper spill response must be taken to curtail and separate the spilled oil from the marine for impact minimization. However, marine oil spill response would generate a large volume of oily wastewater that needs effective treatment. The ineffective treatment and discharge of oily wastewater would pose secondary adverse impacts to the environment. For example, insufficiently treated oily wastewater can cause air pollution because of the evaporation of light petroleum hydrocarbons and jeopardize the aquatic environment because of the presence of toxic substances (Jamaly, 2015; Ismail et al., 2020). Thus, stringent discharge regulations must be applied to minimize the harmful effects. The approved daily average discharge limit for oil and grease in Canada is 30 mg/L (Al-Dulaimi and Al-Yaqoobi, 2021). According to the United States Environmental Protection Agency (USEPA), the oil and

grease discharge limit is 29 mg/L for monthly average with a maximum daily discharge of 42 mg/L (Souza et al., 2020).

Oil spills in the Arctic Ocean are of particular concern since the oil spill response in this region is much more challenging than temperate regions. The specific challenges are mainly due to the unique harsh environments in the Arctic, such as lack of sunlight in winter, strong wind, cold temperature, remoteness, and the presence of sea ice (Nordam et al., 2019). On the other hand, global climate change has already altered the ice cap coverage in the Arctic and led to increased opportunities for marine activities (e.g., oil exploration and transport, tourism), which would potentially increase the risk of oil spills (Crépin et al., 2017; Wilkinson et al., 2017). In addition, the drastic reduction of ice coverage in the Arctic may result in faster spread of spilled oil and higher risks of shoreline exposure when oil spills occur (Nordam et al., 2017). Considering the lack of sufficient infrastructure and remoteness in the Arctic, it is highly desirable to have on-board systems in response vessels for treatment of oily wastewater generated from oil spill response operations.

The oil can exist in wastewater in three different forms, as free oil (the diameter of oil droplets > 150 μm), dispersed oil (20–150 μm), and emulsified oil (< 20 μm) (Yu et al., 2020). The most challenging part for treating oily wastewater is the presence of stable oil-water emulsion. There are various oil-water separation technologies available for breaking oil-water emulsions (i.e., demulsification), including chemical treatment, biological process, and membrane filtration. However, these demulsification methods are associated with different drawbacks, such as secondary contamination caused by chemical reagents, slow biological treatment process, and high operational costs due to short membrane life (Oliveira et al., 2017). In terms of marine oil spill response, the effective separation of oil from oil-water emulsion is of critical importance for

greatly enhancing the response capacity of response vessels that have limited storage space. However, the lack of technologies for effective oil-water separation and at-sea disposal of decanted water becomes a bottleneck in response operations in many countries such as Canada, USA and China (Mohammadiun et al., 2021). Therefore, it is necessary to explore new technologies that could be more efficient in demulsification.

In recent years, NBs and MBs-based gas flotation technology has been used for wastewater treatment such as surface water purification (Kyzas and Matis, 2018) and groundwater remediation (Xia and Hu, 2016). Gas flotation-based technologies may have great potential in treating oily wastewater due to the compact footprint of equipment required, high separation efficiency, and limited sludge production (Yu et al., 2017). Unlike some other conventional wastewater treatment methods (e.g., biological processes), gas flotation-based technology is more sustainable and environmentally friendly without resulting in direct greenhouse gases (GHG) emissions or significant secondary pollution (Campos et al., 2016). MBs and NBs can adsorb oil droplets to form light flocs that can float to the wastewater surface due to decrease in the overall density (Bai et al., 2011). The separation of oil droplets and water can be achieved by skimming off the floating oil flocs on the liquid surface (Saththasivam et al., 2016). Based on the recent advancements in the gas flotation-based wastewater treatment, there is a need for a comprehensive review of MBs and NBs-based gas flotation technologies to help better understand the mechanisms behind the oil-water separation process and its potential for use in new applications (e.g., decanting of oily wastewater generated from marine oil spill response). The main objectives of this review are (a) to introduce the mechanisms and properties of MBs and NBs as well as their generation methods, (b) to summarize the types of MBs and NBs-based gas flotation system and their design

considerations, and (c) to discuss the influential factors affecting oil-water separation as well as future development needs in MBs and NBs-based gas flotation.

2.2 Properties of MBs and NBs

A number of fundamental bubble properties may influence the use and effectiveness of MBs and NBs in gas flotation. These include bubble size, specific surface area, zeta potential (ZP), rising velocity, internal pressure, and bubble stability.

2.2.1 Bubble size

2.2.1.1 Size definition

There are different definitions of MBs and NBs. For example, the diameter of MBs was defined to be less than 50 μm by Kobayashi et al. (2011). According to Agarwal et al. (2011), the size of MBs is in the range of 10 to 50 μm in diameter. However, Pérez-Garibay et al. (2012) categorized MBs with a diameter of 30–100 μm. Ross et al. (2019) suggested that the size of MBs is typically 30–70 μm in diameter. Although a consensus on the size of MBs has not been reached, it is generally accepted that MBs fall within a size range of 1–100 μm.

As for NBs, Agarwal et al. (2011) categorized NBs as those with a diameter of less than 200 nm. Attard (2016) classified NBs as those within a range of 10 to 500 nm. Rameshkumara et al. (2019) mentioned that NBs are gaseous cavities having the size of 100–800 nm in diameter. In recent studies, Yasuda et al. (2019) stated that NBs have a diameter of less than 1 μm, and Kim et al. (2020) classified NBs as ultrafine bubbles with a diameter of 100 nm–1 μm. Overall, the size of NBs is in the order of nanometers as shown in Figure 2.1.

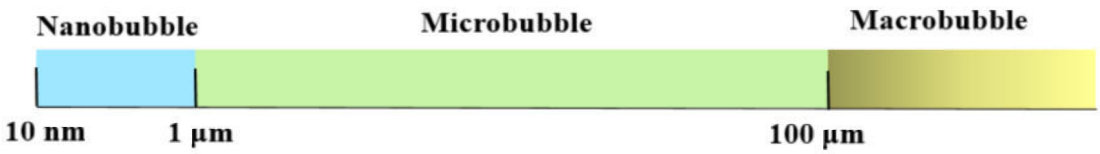

Figure 2.1 Summarized diameter range of MBs and NBs

2.2.1.2 Size measurement

Different techniques have been developed and used to measure the bubble size and its distribution. Li et al. (2016b) used a microscope equiped with an image processing software called Image-Pro Plus to determine the distribution of micro- and macro-bubbles in the range of 10–150 µm. ImageJ ™ is also a widely used software to process images obtained from microscope observation (Gonzalez-Galvis and Narbaitz, 2020). A microscopic photo including a MB of about 12 µm (upper right) and NBs with diameters of 100–500 nm is shown in Figure 2.2. Although visible images could be generated, it was a tedious task as the field of view under a microscope is limited (Temesgen et al., 2017). Meegoda et al. (2018) determined the distribution of nano- and micro-bubbles over a size range of 0.3 nm to 10 µm using a Dynamic Light Scattering (DLS) instrument (Zetasizer Nano ZS, Malvern Instruments Ltd.). da Cruz et al. (2016) used laser diffraction (LD) method (Mastersizer 2000SM device, Malvern Instruments Ltd.) to determine the average bubble size generated in EF system. Compared with LD, DLS can be used to detect samples with much smaller particle sizes (Badger, 2019). An acoustic bubble spectrometer was applied by Rehman et al. (2015) to measure the bubble size distribution over a size range of 80–450 µm. According to Desai et al. (2019), acoustic spectrometry is able to detect smaller bubbles in comparison to LD and optical techniques.

Figure 2.2 Photo of MBs and NBs from a phase-contrast microscope (provided by K. Takahashi, personal communication, 2022)

2.2.1.3 Bubble size impact factor

Many studies have been conducted to investigate the effects of different factors on bubble size. According to Wu et al. (2012), temperature has a significant effect on bubble size because it can greatly affect the coalescence of bubbles. Higher temperatures led to the formation of larger bubbles. Gas flow rate and gas pressure are two other important factors affecting bubble size (Meegoda et al., 2018). Nazari et al. (2020b) investigated the effect of air flow rate on the size of bubbles generated from a Venturi tube, and they obtained smaller bubbles when a high air flow rate (increasing dissolved gas) was applied. Temesgen et al. (2017) concluded that smaller bubbles would be produced under higher pressure due to increased air density. Calgaroto et al. (2014) found that to some extent bubble size is dependent on the magnitude of ZP and the maximum bubble size was achieved at the isoelectric point. Table 2.1 lists the aforementioned impact factors, operating conditions, and the related bubble size measurement methods.

Table 2.1 Different factors affecting bubble size

Factors		Bubble size	Size measurement	Operating conditions	Reference
Solution temperature (°C)	20	200 nm	Mastersizer 2000 (Malvern Instruments)	NA	Ahmadi and Khodadadi Darban, 2013
	25	230 nm			
	30	265 nm			
	35	310 nm			
	40	360 nm			
Gas pressure (kPa)	482	66.5 µm	High-speed high-resolution flare camera + ImageJ software	The size measurements were performed with tap water and conducted under room temperature = 20 ± 2 °C	Gonzalez-Galvis and Narbaitz, 2020
	551	54.4 µm			
	620	47.7 µm			
Gas flow rate (L/min)	0.1	629 nm	Mastersizer 2000 (Malvern Instruments)	Liquid temperature = 32 °C, pH = 8, gas pressure = 325 kPa	Nazari et al., 2020b
	0.18	482 nm			
	0.25	390 nm			
	0.33	300 nm			
	0.4	243 nm			
pH	2	130 nm	Zetasizer Nano ZS – Zen3600 (Malvern Instruments)	Gas pressure = 455 kPa, bubbles were produced in 10^{-2} mol/L NaCl solution	Calgaroto et al., 2014
	4	570 nm			
	6	715 nm			
	8	420 nm			
	10	300 nm			

Note: NA = not available

2.2.2 Specific surface area

The specific surface area of MBs and NBs are larger than that of the conventional macro-bubbles and it can be calculated by the following equations (Li et al., 2013):

$$S = 4\pi r^2 \tag{2.1}$$

$$V = 4/3\,\pi r^3 \tag{2.2}$$

$$S/V = 3/r \tag{2.3}$$

Where S is the surface area (m^2), V is the volume (m^3), and r is the radius of the bubble (m). From the above equations, it can be found that the specific surface area (surface area per unit volume) will be larger for bubbles with a smaller radius. For example, the specific surface area of NBs with radius of 10 nm is 1000 times larger than that of MBs with radius of 10 μm and is 10,000 times larger than that of macro-bubbles with radius of 1 mm. According to Swart et al. (2020), the specific surface area is in the order of 10^5 m^{-1}. Therefore, the large surface area of MBs and NBs can sequester more unwanted particles in the solution than macro-bubbles for improved adsorption performance.

Calgaroto et al. (2015) investigated the flotation of fine quartz particles (mean diameter of 32 μm) with and without NBs (200–720 nm), and they found that the recovery of quartz particles was increased from 44% to 64% with the assistance of NBs. Similarly, Nazari and Hassanzadeh (2020a) observed around 27% improvement in quartz particles separation in the presence of NBs (mean diameter of 247 nm). Rosa and Rubio (2018) successfully increased the separation of quartz particles (mean diameter of 50 μm) by 23% with NBs (150–200 nm). Etchepare et al. (2017a) improved the oil separation efficiency from 72.6% with MBs (30–40 μm) alone to 83.9% with MBs and NBs (150–350 nm). Figure 2.3 shows that the contaminant separation efficiency increases with the addition of NBs in the gas flotation system.

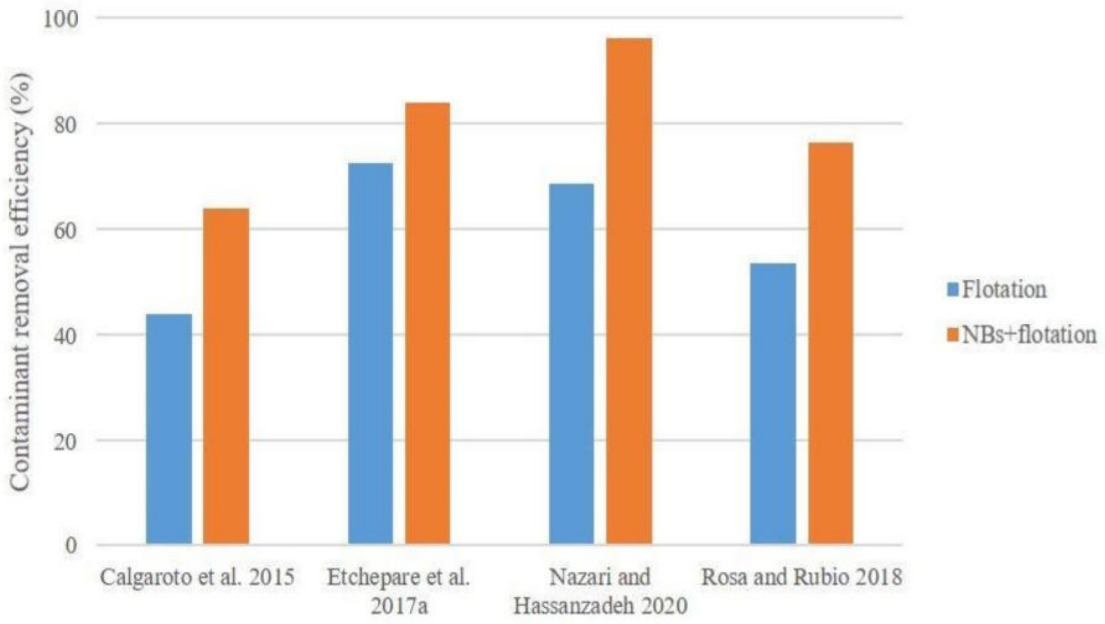

Figure 2.3 Contaminant separation efficiency with and without NBs

2.2.3 Zeta potential

ZP is the electrical potential of any particles (e.g., gas bubbles or oil droplets) in suspension which shows repulsive or attractive forces between themselves (Gurung et al., 2016). It is formed at the particle-liquid interface. The stability of the colloidal dispersions can be represented by the magnitude of ZP. A higher value of absolute ZP indicates that the dispersion or solution is more stable because it has stronger resistance to agglomeration (Shangguan et al., 2018). Generally, bubbles are negatively charged in distilled water because of the adsorption of hydroxyl ions (OH^-) at the gas-liquid interface (Bui et al., 2019).

Table 2.2 summarizes some studies investigating the effects of various factors (gas type, gas pressure, solution pH, and the addition of surfactant) on ZP. For example, ZP is affected by the type of gas used to form bubbles. High ZP of MBs and NBs can be achieved using oxygen and nitrogen as the injection gas compared with other types of injection gas including carbon dioxide,

xenon, and air (Ushikubo et al., 2010a). Similarly, Meegoda et al. (2018) used ozone, oxygen, air and nitrogen to generate NBs in deionized water (DI) and the highest ZP was observed in ozone bubbles followed by oxygen, air, and nitrogen. They concluded that the difference in ZP is caused by different gas diffusion rates and gas solubility, which impact the ability of OH^- ions formation at the bubble surface. Jia et al. (2013) investigated the effects of surfactant type and concentration on ZP of air bubbles in aqueous solution. They concluded that addition of cationic surfactant reduced the negative charge of ZP and even changed the negative charge into positive, however, the addition of anionic surfactant helped make the ZP more negative.

Table 2.2 Different factors affecting zeta potential

Factors		ZP (mV)	Reference
Gas type	Nitrogen	-19.8	Meegoda et al., 2018
	Air	-21.3	
	Oxygen	-22.4	
	Ozone	-27.0	
Pressure (kPa)	138	-0.3	Ahmed et al., 2018
	207	-3.8	
	275	-10.0	
	345	-15.2	
	414	-22.5	
pH	5	-18.2	Kim and Kwak, 2017
	7	-21.8	
	9	-28.1	
	11	-30.5	
Anionic surfactant concentration (ppm)	50	-37.8	Jia et al., 2013
	100	-42.0	
	150	-52.2	
	200	-64.1	

Note: ZP = zeta potential

2.2.4 Rising velocity

The rising velocity (V_r) of MBs and NBs can be expressed by the equation of Stoke's Law, which states that the rising speed of bubbles is directly proportional to bubble size and inversely proportional to the viscosity of surrounding liquid (Zhang et al., 2019):

$$V_r = \frac{d^2 g(\rho_l - \rho_g)}{18\mu_l} \tag{2.4}$$

Where d is the bubble diameter (m), g is the gravitational acceleration constant (9.8 m/s^2), μ_l is the viscosity of the surrounding liquid (Pa·s), ρ_g is the density of gas bubble (kg/m^3) and ρ_l is the density of the surrounding liquid (kg/m^3).

This equation is valid only for sphere shape and same size of bubbles in laminar flow. However, it is impossible to achieve all these conditions in a real-world situation (Atarah, 2011; Saththasivam et al., 2016). The rising velocity is dependent on the physical properties of the liquids and the diameter of bubbles. Because of their small diameter, MBs and NBs tend to have a slow rising velocity, enabling much longer stagnation under water surface compared with other conventional large bubbles (Tsuge, 2014; Shangguan et al., 2018). Thus, MBs and NBs will spend more time under water which leads to higher rate of collision; hence, more opportunities to adsorb oil particles during the treatment process. Bubble rising velocity is commonly measured using high-speed photography combined with digital image analysis technique (Liu et al., 2016). Swart et al. (2020) listed that when the diameter of MBs is in the range of 10–120 μm, the rising velocity is from 1 to 12 mm/s. As for NBs, the rising velocity of NBs with a diameter of 100 nm is 2.7 nm/s according to the calculation by Alheshibri et al. (2016).

The low rising velocity means that NBs alone are not effective for flotation (Gurung et al., 2016; Calgaroto et al., 2015). According to Azevedo et al. (2016), the rising velocity of MBs in DI water was enhanced from 0.062 cm/s to 0.081 cm/s with the help of NBs. They concluded that

the collision and attachment of contaminant particles to MBs were facilitated by NBs. In addition, Calgaroto et al. (2015) indicated that the most important mechanisms of NBs aiding the flotation with MBs are: the contact angle between contaminant particles and MBs was enhanced, and the aggregation of particles was induced. It was reported that the combination of MBs and NBs has a high potential in separating pollutants from wastewater (Kyzas et al. 2021).

2.2.5 Internal pressure

The relationship between the size of bubble and its internal pressure can be illustrated by the Young-Laplace equation (Tsuge, 2014; Faghri and Zhang, 2020):

$$\Delta P = 4\sigma/d \tag{2.5}$$

Where ΔP is the pressure difference between the internal gaseous bubble and the surrounding bulk liquid (Pa), σ is the surface tension (N/m) of the liquid and d is the bubble diameter (m).

The gas pressure inside the bubble would increase when the bubble size decreases in the aqueous solution (Agarwal et al., 2011). High internal pressure is a driving force that leads to gas diffusion from the high partial pressure area inside of the bubble to the low partial pressure area in the surrounding liquid. Consequently, the size of MBs will be reduced due to the internal gas reduction and the internal pressure will become higher, which causes further bubble shrinkage until the MBs disappear (Xu et al., 2008). However, it was claimed that when the diameter of MBs is beyond 50 μm, the bubbles will swell and rise to the water surface and then burst; otherwise, they will shrink under water (Meegoda et al., 2018). In the case of NBs, their size under water surface remains almost unchanged once they are produced, which means NBs are highly resistant to gas diffusion as shown in Figure 2.4. According to Ohgaki et al. (2010), the low gas diffusivity

of NBs is based on the strong hydrogen bonds on the surface that increase the surface tension of NBs (e.g., 2 times higher than the normal value), restraining the internal gases from permeating through the interfacial film of NBs. The low buoyancy of NBs prevents them from rising to the water surface. Instead, they are subjected to Brownian motion resulting in random movement under water (Farid et al. 2022). The detailed movements of MBs and NBs in the liquid and their interactions need to be further investigated.

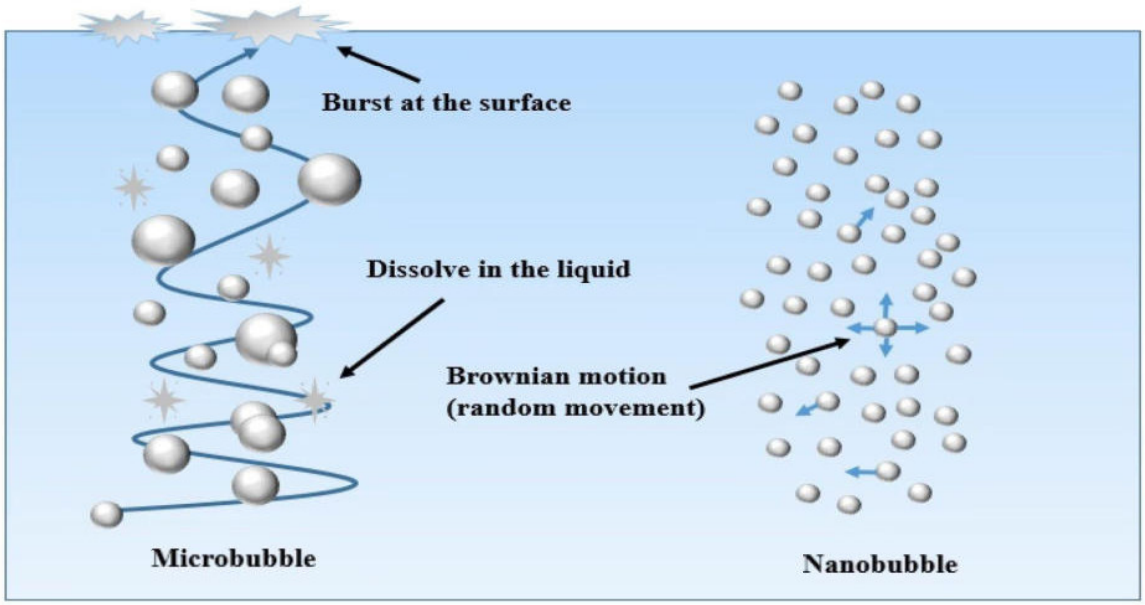

Figure 2.4 Schematic diagram showing the behavior of MBs and NBs under water (modified from Agarwal et al. 2011)

2.2.6 Stability of NBs

The characteristic distinguishing NBs from other types of bubbles is that NBs can last for a long period of time under aqueous solution without bursting out (Rameshkumara et al., 2019). Etchepare et al. (2017b) used a centrifugal multiphase pump to generate air NBs and summarized that the NBs can be stable in the aqueous solution for more than two months with almost unchanged bubble concentration and mean size (Table 2.3). Oh et al. (2015) investigated the

stability of hydrogen NBs in gasoline fuel and concluded that there was no notable change in the concentration and mean diameter of NBs for 121 days. Michailidi et al. (2020) reported that both air and oxygen filled NBs can remain stable for 3 months or even longer. NBs are remarkably stable due to the following reasons: (a) the formation of micrometer-sized clusters helps to prevent the diffusion of gas inside of the bubbles (Ulatowski et al., 2019); (b) the electrostatic repulsive forces generated by the strong absolute ZP between neighboring NBs could stop bubbles from aggregation and coalescence (Ushikubo et al., 2010b); (c) the gas outflux and the gas influx are at equilibrium when the NBs exist in a saturated solution (Azevedo et al., 2016); (d) the high resistance of gas diffusion at the bubble interface due to its different structure (e.g., strong hydrogen bonds) also contributes to the stability of NBs (Wang et al., 2013).

Table 2.3 The change of NB concentration and mean diameter in a specific period of time

Initial stage		Final stage		Duration	Reference
NB concentration (particles/mL)	Mean diameter (nm)	NB concentration (particles/mL)	Mean diameter (nm)	(day)	
$(3.47 \pm 0.39) \times 10^8$	88.50 ± 9.59	$(2.94 \pm 0.16) \times 10^8$	110.00 ± 4.58	1	Oh and Kim, 2017
$(11.25 \pm 2.77) \times 10^8$	159.00 ± 31.91	$(10.87 \pm 0.64) \times 10^8$	146.80 ± 8.11	121	Oh et al., 2015
6.0×10^8	150-200	5.1×10^8	300	60	Etchepare et al., 2017b

2.3 Generation of MBs and NBs

As shown in Figure 2.5, several methods can be used to generate NBs and MBs. The strengths and weaknesses of some widely used bubble generation methods are listed in Table 2.4.

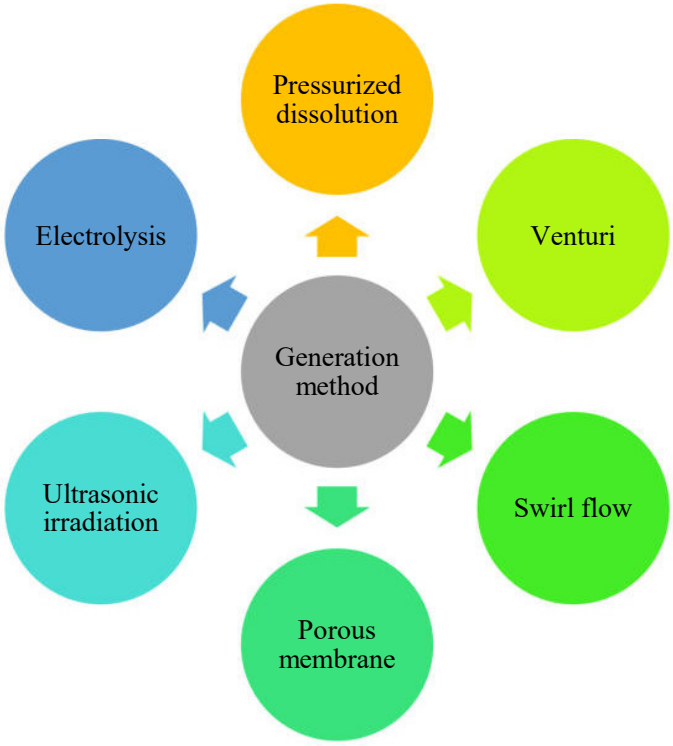

Figure 2.5 Bubble generation methods

2.3.1 Pressurized dissolution type

For bubble generation by pressurized dissolution, the gas will be dissolved in water under high pressure (typically at 3–4 atm) within a saturator vessel to create a supersaturated condition (Agarwal et al., 2011; Parmar and Majumder, 2013). When this supersaturated water is introduced into a tank of water through a nozzle under atmospheric pressure (Figure 2.6), MBs are rapidly formed as the gas escapes (Arumugam, 2015). Maeda et al. (2015) summarized that by increasing

the dissolved gas concentration in the liquid phase, the mean diameter and number density of bubbles will also be increased. Norarat et al. (2019) used a bubble generator based on the pressurized dissolution method and investigated the effect of its operation time on bubble concentration. They found that the increased operation time led to higher bubble concentration and the bubble size distribution shifted to smaller sizes under longer operation times.

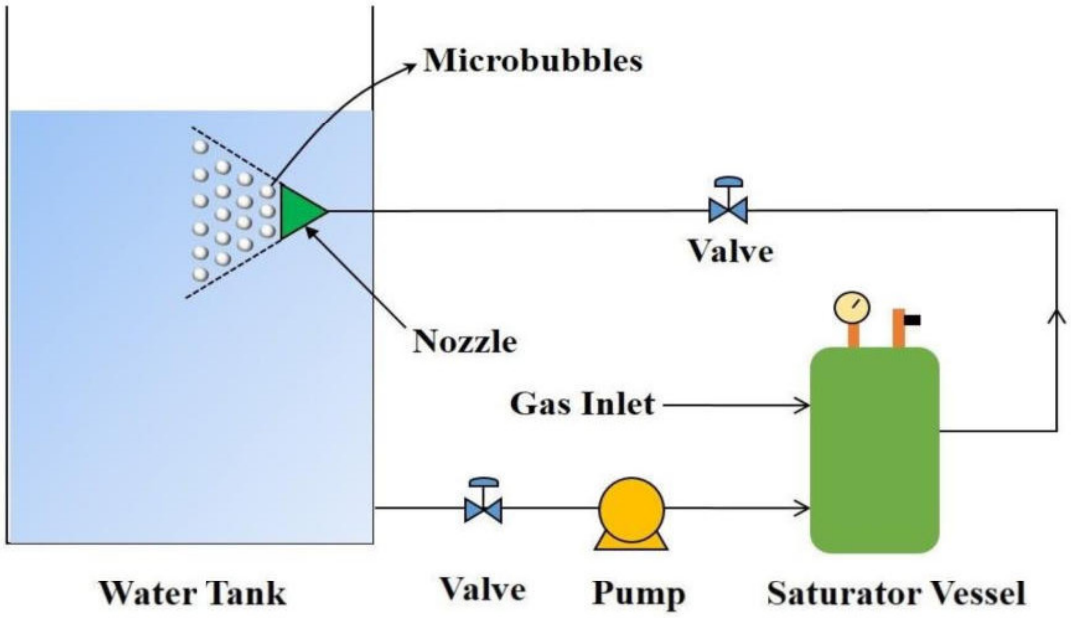

Figure 2.6 Pressurized dissolution type bubble generator (modified from Arumugam, 2015)

2.3.2 Venturi type

Venturi based bubble generation involves three major components: a converging inlet, a throat, and a diverging outflow as shown in Figure 2.7 (Zhao et al., 2017; Huang et al., 2020). It includes the injection of gas into the venturi tube along with water through the converging inlet (Parmar and Majumder, 2013) or at the throat section (Li et al., 2017; Huang et al., 2020). Zhao et al. (2017) investigated the bubble generation mechanisms in a venturi type bubble generator and they found that there was a pressure decrease in the throat region which leads to the increasing

bubble velocity. After that the air bubbles are rapidly decelerated when entering the diverging outflow section due to the pressure recovery. The relative flow velocity difference between liquid phase and air bubbles generates a shock wave with high shear forces that cause bubble deformation and the collapse of large bubbles into a large number of tiny bubbles (Zhao et al., 2017; Tsuge, 2014). MBs with diameter less than 100 μm can be formed by this method (Agarwal et al., 2011). Li et al. (2017) showed that the divergent angle is a significant parameter influencing the performance of venturi type bubble generator. The produced bubble size decreases with an increase in divergent angle. Huang et al. (2020) indicated that liquid flow rate is the main parameter controlling the bubble size and distribution. A more uniform bubble size distribution can be obtained by increasing the liquid flow rate.

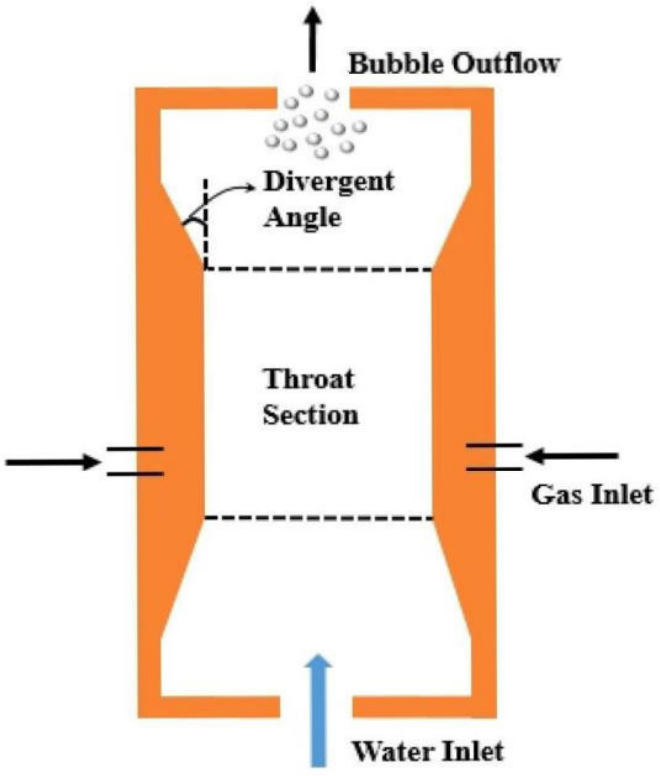

Figure 2.7 Venturi type bubbe generator (modified from Zhao et al., 2017; Li et al., 2017)

2.3.3 Swirl flow type

Bubble generation by swirl flow involves the pumping of pressurized water into a cylindrical container to form a spiral flow pattern as shown in Figure 2.8 (Parmar and Majumder 2013). The rotary liquid flow could lead to low pressure in the central axis part that draws in gas from the bottom of the cylindrical container into the water vortex (Agarwal et al., 2011; Arumugam, 2015; Ulatowski and Sobieszuk, 2020). Tiny bubbles are generated in the top part of the container by high shearing force in the process of vortex breakdown (Parmar and Majumder, 2013). Alam et al. (2018) used a computational fluid dynamic simulation method to study the performance of a swirl flow bubble generator that produced MBs with an average diameter of 50 μm. They found that the number of MBs produced is dependent on the air mass flow rate, and the lower mass flow rates produced a higher number of MBs.

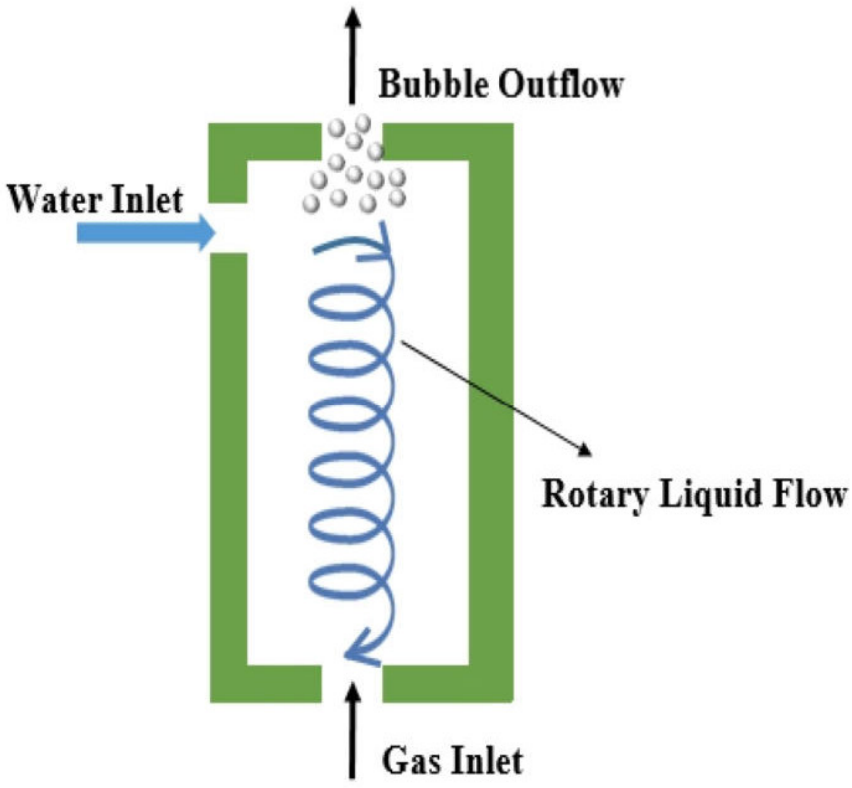

Figure 2.8 Swirl liquid flow type bubble generator (modified from Parmar and Majumder, 2013)

2.3.4 Porous membrane type

In porous membrane bubble generation, compressed gas is introduced from the outside of the membrane through its pores. A liquid phase flows inside the membrane and generates shear force to form bubbles on the membrane surface (Khirani et al., 2012; Ulatowski and Sobieszuk, 2020). Xie et al. (2021) designed a MBs generation system using a commercial porous ceramic membrane. In their experiments, the liquid phase was pumped into the inner of membrane which created shear flow to disperse nitrogen to MBs. They investigated the effect of liquid flow velocity on MBs size and found that the increase of liquid flow velocity led to higher wall shear force in the membrane which accordingly decreased the MBs size. Also, they concluded that membrane pore size is an important factor controlling MBs size, while smaller pore diameter results in smaller bubble generation (Xie et al., 2021). Khirani et al. (2012) investigated MBs formation through tubular ceramic membranes using different continuous phases (water / heptane), different dispersed phase (air / nitrogen) and different membrane materials (alumina oxides / zirconium oxides). However, they summarized that smaller membrane pore size will lead to bigger bubble size which is contrary to the conclusion brought up by Xie et al. (2021). Moreover, they indicated that the use of more hydrophobic membrane surface favors the generation of smaller MBs.

2.3.5 Ultrasonic irridation type

Yasuda et al. (2019) formed NBs in the size range of 90–100 nm diameter by irradiating ultrasound to ultrapure water. A high density of NBs could be achieved by increasing the ultrasonic power and irradiation time and decreasing the ultrasonic frequency. Xu et al. (2008) used two types of surfactants including Sodium dodecyl sulfate (SDS) and L-150A (10% ethanol, 38% sucrose

laurate ester and 52% water) for generating MBs by sonication. Based on their results, the use of 1% SDS yielded larger bubble diameter of 46 μm compared to that of 26 μm using 1% L-150A. Besides, the volumetric bubble concentration was 8.3×10^6/mL when using SDS as surfactant while it was 2.5×10^7/mL when using L-150A. Lee et al. (2020) studied the effect of dissolved gas concentration on NB generation by ultrasonic irradiation. They used an ultrasonic horn booster at 20 kHz to irradiate the ultrasound for 10 min in three types of DI water namely under-saturated, saturated, supersaturated. They found that with the increase of the dissolved gas concentration, the surface tension of DI water decreased, causing a reduction in the concentration of NBs.

2.3.6 Electrolysis type

Oxygen and nitrogen bubbles can be produced by electrolysis at both the anode and cathode respectively due to redox reactions (Favvas et al., 2021). Lucero et al. (2017) performed experiments to evaluate the effect of NaCl concentration, current density, and electrode distance on MBs generation rate. Among all the parameters, current density directly controlled the generation rate, and higher current density resulted in faster bubble generation. The power requirement of the electrolysis process was decreased by the addition of NaCl and narrowing the electrode distance. Ulatowski et al. (2021) also investigated the influence of salt concentration and electrolysis time on the mean diameter of nitrogen and oxygen bubbles formed by electrolysis. It was observed that the diameter of bubbles increased with the increase in salt concentration, while the extension of electrolysis time only affected the hydrogen bubble size, which tended to be smaller with the increase of electrolysis time. In the process of electrolysis, the mean diameter of bubbles decreased at first and then reached equilibrium after an hour (Chandran et al., 2015).

Table 2.4 Comparison of different bubble generation methods

Methods	Strength	Weakness	Reference
Pressurized dissolution	• Stable and uniform MBs with high bubble density can be generated • Simple system	• High energy consumption • Probability of blockage of air supply due to circulation of contaminated water	(Maeda et al., 2015; Tamura et al., 2014)
Venturi	• Less maintenance (no internal moving parts) • Low power consumption • Easy to install due to its simple structure • High efficiency and good reliability	• The generated bubble size differs from tens of microns to millimeters (lack uniformity)	(Huang et al., 2020; Kobayashi et al., 2022)
Swirl flow	• Highest gas holdup and gas transfer comparing with other methods	• Strong shear flow causing breakage of the product • Complicated structure	(Wang et al., 2020; Terasaka et al., 2011)
Ultrasonic method	• Can generate mono-dispersed fine MBs • Short bubble generation time • Compact bubble generator with simple operation	• The generated bubble density is not high	(Maeda et al., 2015; Yasuda et al., 2019)

2.4 Gas flotation

There are currently three principal gas flotation technologies, including dissolved gas flotation (DGF), IGF, and electrolytic flotation (EF). They have been adopted for oily wastewater treatment, and Table 2.5 lists some application examples. The advantages and limitations of the three flotation systems in wastewater treatment are listed in Table 2.6.

Table 2.5 Application of gas flotation system for treating oily wastewater

Flotation type	Bubbles type	Oil separation	Remark	Reference
DAF	Macro-bubbles	98%	Light crude oil was used to prepare emulsion with different initial oil concentrations (e.g., 850 ppm, 1130 ppm); flotation time varied from 10 min to 4 h for different flotation process	Rajak et al., 2015
	MBs and NBs	>99%	1.6 g/L of medium crude oil emulsion was used to conduct the experiments; Dismulgan V3377 was used to destabilize the emulsion before flotation; 5 min of flotation with a recycle ratio of 25%	Etchepare et al., 2017a
	MBs	95%	Motor oil was used to generate emulsion with a concentration of 15 g/L; biosurfactant produced from the bacteria *Pseudomonas aeruginosa* was used to facilitate the coalescence of contaminant particles	Silva et al., 2019
	NA	85%-95%	Wastewater with 7-15 g/L biodiesel; acidification and alum coagulation were applied before DAF; retention time in the flotation cell was 7 and 9 min for 20% and 40% recycle ratio	Rattanapan et al., 2011
Induced air flotation (IAF)	Macro-bubbles	89%	Oily wastewater with initial oil concentration of 30, 100, and 800 ppm; optimal flotation time was 20-25 min	Mohammed et al., 2013
	NA	93%	Emulsion with 500 mg/L initial oil concentration; aluminum sulfate was used for the coagulation process; flotation time was 10 min	Hoseini et al., 2015
	Macro-bubbles	>85%	Three types of stabilized oily wastewater which contain 1 g/L cutting oil, 3 g/L lubricant oil, and 5 g/L palm oil; optimum alum dosages:150 mg/L for cutting oil, 400 mg/L	Chawaloesphonsiya et al., 2019

			for lubricant oil, and 800 mg/L for palm oil; 0.1-1 L/min of air flow rate (optimum 0.3 L/min)	
EF	NA	99%	Synthetic emulsions with 500 mg/L crude oil, 15% surfactant, and saline water; maximum oil separation achieved after 35 min; increasing current density and NaCl concentration increase oil separation efficiency	Hassan et al., 2015
	NA	99%	500 mg/L of emulsified lubricant oil used; aluminum electrodes preferred than iron electrodes in order to attain a higher separation efficiency; 99% separation efficiency achieved in 10 min; separation efficiency increased with electrode size and the gap between electrodes	Mohammed and Al-Gurany, 2010
	NA	85%	Bor oil (a common cutting oil) was used to prepare oily wastewater; maximum oil separation efficiency was obtained when the highest voltage (15V) was applied	Genç and Goc, 2018

Note: NA = not available

Table 2.6 Summary of different types of gas flotation systems

Types of flotation	Advantage	Disadvantage	Reference
DGF	• Low maintenance cost (non-moving parts) • Easy to operate • Widely used technology with huge market, high maturity, and reliable performance	• High equipment footprint and capital cost • Not suitable for treating wastewater with high inlet concentration • Bubble quantity generated is low due to the limitation on saturation	Saththasivam et al., 2016; Ebrahiem et al., 2021
IGF	• Low retention time resulting in a compact footprint • Low capital cost • High inlet concentration can be accepted • No compressor needed (saving the running cost)	• High maintenance cost due to wear and tear of impellers • If diffusers are used to introduce gas, they might be clogged leading to less effectiveness of the system	Ebrahiem et al., 2021; Piccioli et al., 2020
EF	• Uniform mixing of gas bubbles and wastewater can be achieved • Operating conditions (e.g., gas production) can be easily controlled • Lack of requirement for chemicals additives	• Continuous supply of electricity is required for bubble generation • Maintenance and replacement of anodes on regular basis which may lead to high cost	Khalek et al., 2019; Kyzas and Matis, 2016

2.4.1 Dissolved gas flotation

DGF is the most commonly used technique for treating industrial wastewater especially oily wastewater (Kyzas and Matis, 2018). In the DGF process (Figure 2.9), fine gas bubbles are formed due to the pressure reduction in the pre-saturated aqueous solution when it passes through needle valves or orifices (Fonseca et al., 2017). The generated bubbles have a size range of 20–100 μm diameter (Edzwald, 2010; Brasileiro et al., 2020).

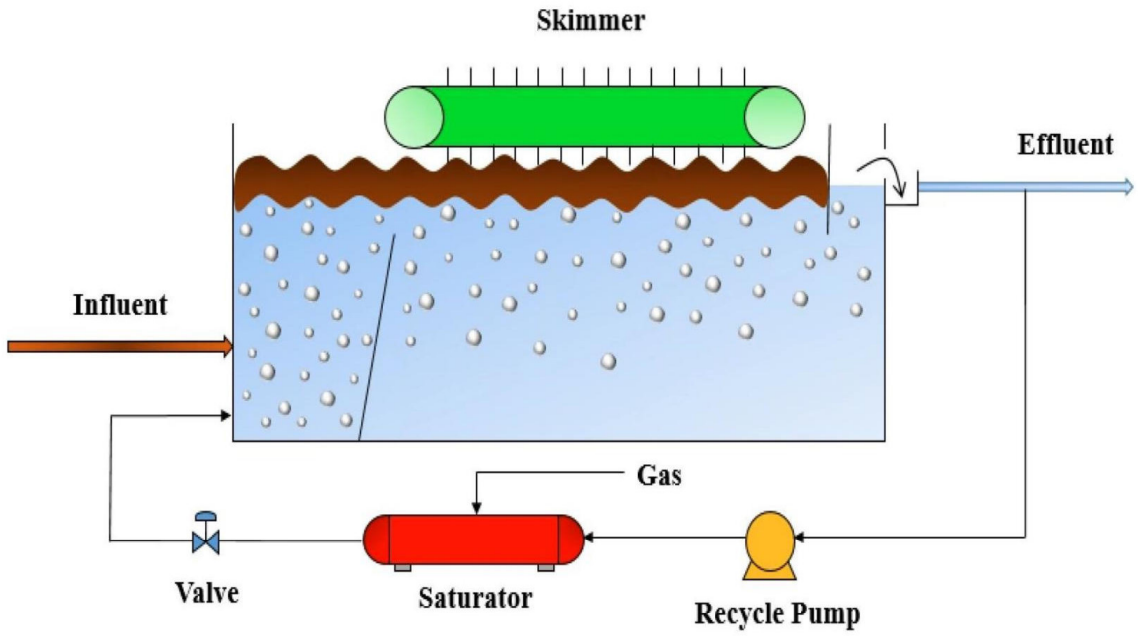

Figure 2.9 Schematic of DGF system (modified from Behin and Bahrami, 2012)

In terms of effectiveness, Rattanapan et al. (2011) stated that DGF is effective to separate liquid or solid particles with low concentrations from aqueous suspension. However, Jaji (2012) noted that the retention time in DGF can be in the range of 20-60 min which makes it infeasible to treat wastewater with high feed flow rates. Furthermore, due to the high retention time, DGF systems are associated with higher equipment footprint and capital costs (Saththasivam et al., 2016).

There are three different liquid flow schemes in the DGF system including full-flow, split-flow, and recycled flow (Figure 2.10). The wastewater stream is entirely pressurized in the saturator vessel in the full-flow scheme, while it is partially pressurized in the split-flow system. The recycled flow DGF system is the most widely used scheme for the flotation treatment process. Only a part (15%–30%) of the treated effluent is pumped into the saturator vessel to be pressurized and then it is recycled back to the flotation tank (Wang et al., 2010). While air is the most commonly used gas for the DGF system, a number of other gases have been used (Table 2.7), such as nitrogen, carbon dioxide, ozone, and methane.

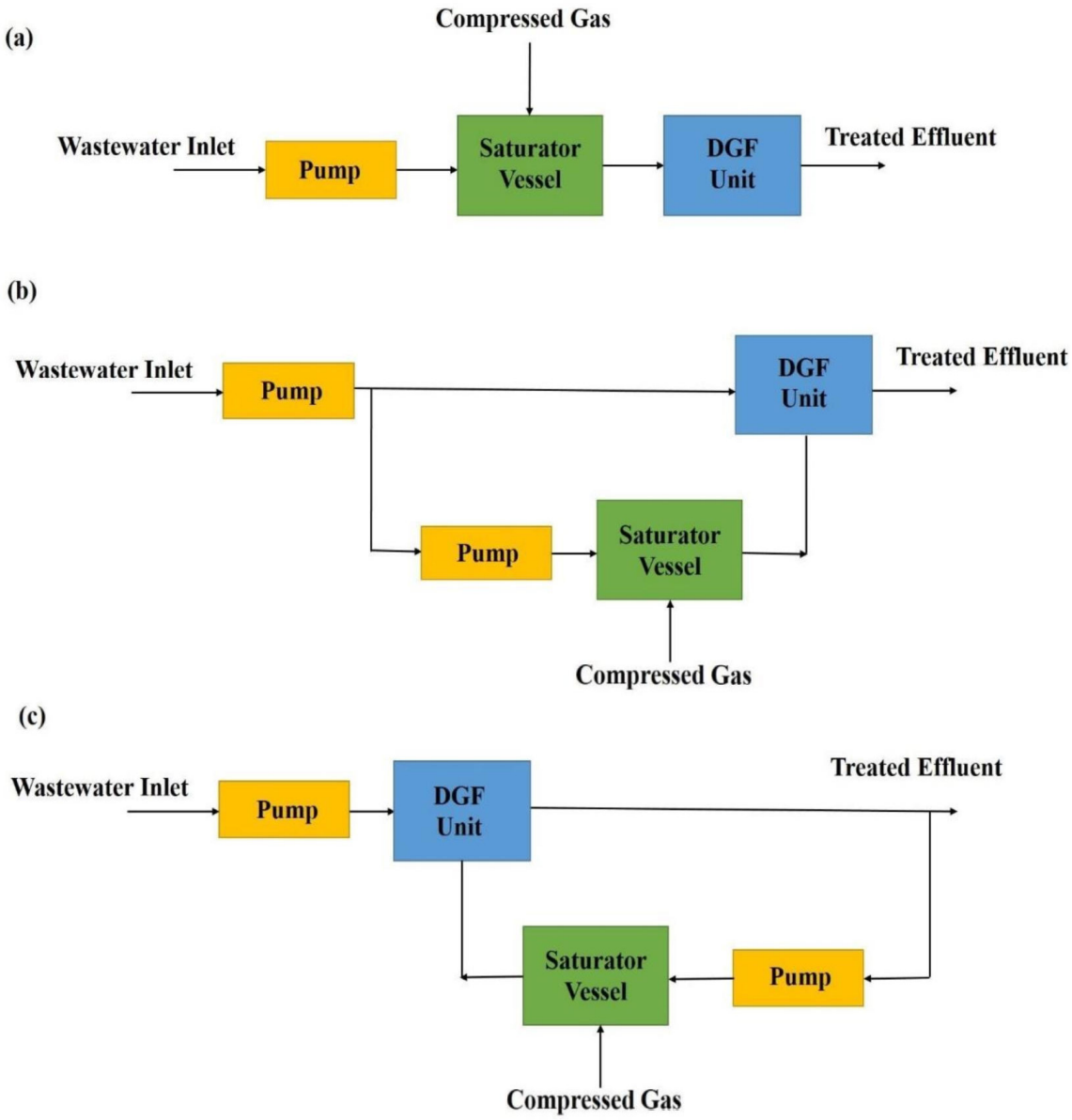

Figure 2.10 Different flow schemes of DGF system, (a) full-flow pressurization, (b) split-flow pressurization, and (c) recycled flow pressurization (modified from Radzi 2016)

Table 2.7 Summary of different gases used in DGF system for wastewater treatment

Gas types	Wastewater	References
Air	Restaurant dishwasher effluent	Wu, 2017
Nitrogen	Produced water	Maelum and Rabe, 2015

Carbon dioxide	Livestock wastewater	Kwak and Chae, 2016
Ozone	Cosmetic wastewater	Wiliński et al., 2017
Methane	Oilfield wastewater	Wang et al., 2010

2.4.2 Induced gas flotation

IGF is also called dispersed gas flotation. It involves turbulent hydrodynamic conditions under which bubbles are generated by mechanical mixing and the dispersion of gas into water phase streams through high-speed impellers or diffusers as described for swirl liquid flow bubble generators (Saththasivam et al., 2016; Prakash et al., 2018). IGF systems (Figure 2.11) have been widely used in treating various types of industrial wastewater from different sources including oil and gas production, pulp and paper mills, and dairy industry (Chebbi et al., 2018; Zasadowski et al., 2014; Al-Maliky, 2010).

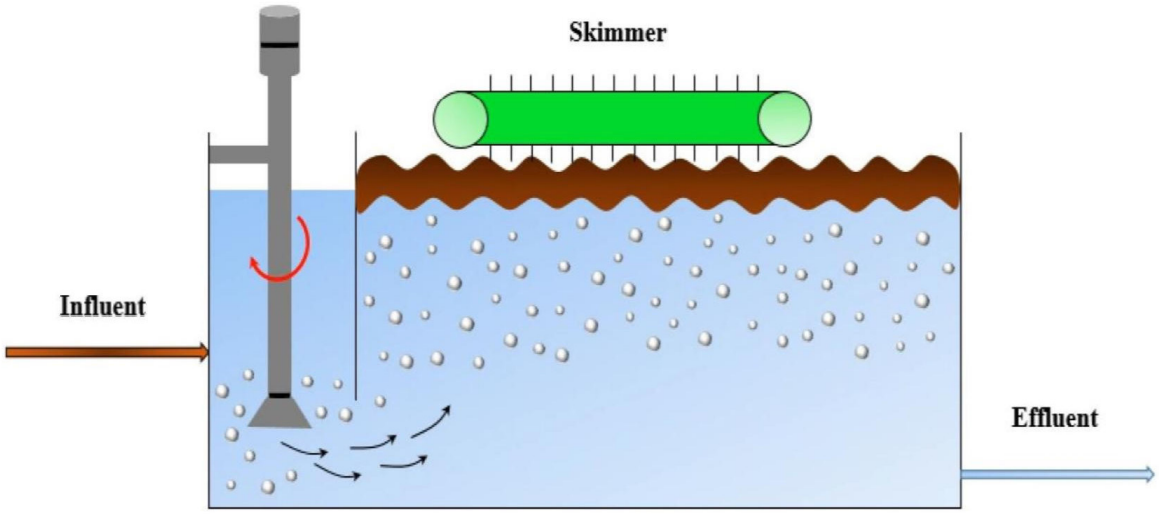

Figure 2.11 Schematic of IGF system (modified from Zasadowski et al., 2014)

A relatively large amount of gas is required for gas bubble formation in IGF systems to produce the high concentration of bubbles and their required size (typically in the range of 700–

1500 μm diameter) (Wang et al., 2010; Radzi, 2016; Naghdi and Schenk, 2016). Due to its considerably lower retention time (normally less than 5 min) than that of the DGF system (Piccioli et al., 2020), the IGF system has a more compact footprint (Wang et al., 2010). While the capital cost of IGF systems is relatively low, maintenance costs may be high due to wear and tear of mechanical parts such as impellers (Saththasivam et al., 2016).

2.4.3 Electrolytic flotation

EF is a wastewater treatment process using fine hydrogen and oxygen bubbles which are generated by electrolytic decomposition of aqueous solutions as illustrated in Figure 2.12 (Eskin et al., 2015). Oxygen is generated at the anode electrode due to the oxidation of water (Eq. 2.6) while hydrogen is released as a result of reduction reaction at the cathode (Eq. 2.7). The overall redox reaction (Eq. 2.8) is also shown below (Mohtashami and Shang, 2019):

$$\text{At the anode: } 2H_2O \rightarrow 4H^+ + O_2 \uparrow + 4e^- \quad (2.6)$$

$$\text{At the cathode: } 4H_2O + 4e^- \rightarrow 4OH^- + 2H_2 \uparrow \quad (2.7)$$

$$\text{Overall reaction: } 2H_2O \rightarrow O_2 \uparrow + 2H_2 \uparrow \quad (2.8)$$

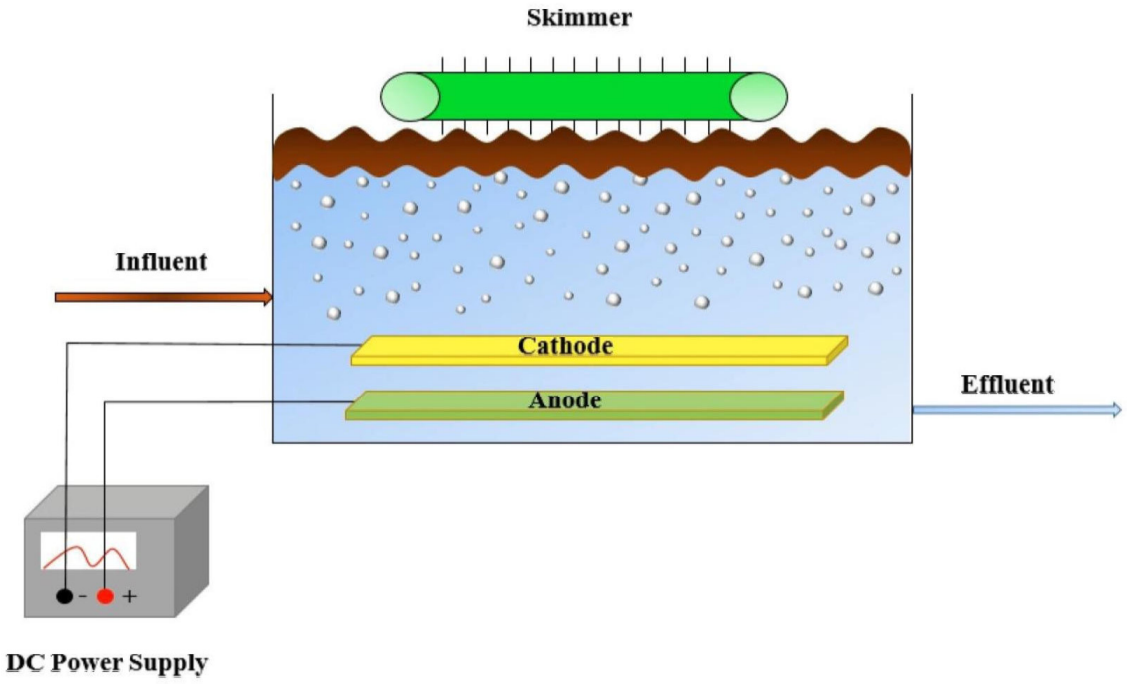

Figure 2.12 Schematic of EF system (modified from Palaniandy et al., 2017)

Kyzas and Matis (2016) listed some advantages of EF including: wastewater and gas bubbles can be well mixed by covering the whole surface area of the flotation cell with electrode grids. The voltage that is needed for electrolysis is within the range of 5–20 V, which makes it safe to operate and a large amount of tiny bubbles can be generated with minimal turbulence. According to Matis and Peleka (2010), coagulation of small particles and liquid droplets occurs without applying any chemical reagents in the EF cell. Alam (2015) suggested that the operating conditions of EF can be easily controlled. While the size of gas bubbles in their test system had an average size of around 20 μm, it was noted that the size and concentration of gas bubbles could be changed by varying the electrical current density.

There are still some disadvantages and challenges existing in the EF treatment method. The main drawback is the amount (and cost) of electrical energy required for continuous bubble formation (Tadesse et al., 2019). Sarkar (2011) noted another major technical issue encountered by EF that is the control of pH, since hydrogen and hydroxide ions are continuously released into

the system. Montes-Atenas et al. (2010) stated that in order to protect the system from overheating because of charge transfer, a cooling system might be needed. In addition, due to the oxidation that takes place at the surface of electrodes, the maintenance and replacement of anodes are regularly required which will increase its total operational cost (Khalek et al., 2019).

2.5 Design parameters for gas flotation

A number of factors need to be taken into consideration in the design of MBs and NBs based gas flotation systems, including gas dissolution, gas holdup, recycle ratio, interfacial tension (IFT), and spreading coefficient.

2.5.1 Gas dissolution

Gas dissolution is a critical factor in the design of effective gas flotation systems. When higher pressure is applied, more gas will be dissolved in the solution which will bring more bubbles into existence when the pressure is reduced back to atmospheric pressure (Atarah, 2011). As indicated by Wang et al. (2022c), large bubbles were generated due to low gas dissolution, which resulted in poor pollutant separation. Haarhoff and Edzwald (2013) reported that liquid salinity has a significant effect on Henry's Law constant, that is much higher in saline water than in freshwater, leading to lower gas solubility in saline water. Fanaie and Khiadani (2020) also showed that gas solubility decreased with salinity increase. Moreover, increasing temperature would increase the Henry's Law constant and thus decrease gas solubility (Dassey and Theegala, 2011).

2.5.2 Gas holdup

In an oil-gas-water system, gas holdup can be represented by the volumetric proportion of the gas phase within the total oil-water emulsion of the flotation unit (Prakash et al., 2018). Gas holdup can be calculated as follows (Kumar et al., 2012):

$$\varepsilon = \frac{\Delta P_0 - \Delta P_1}{\Delta P_0} \tag{2.9}$$

Where ε represents gas holdup, ΔP_1 is the pressure difference between two points (lower and higher ends) of the column after bubble generation (Pa), and ΔP_0 is the corresponding hydrostatic pressure difference between these two points before bubble generation (Pa).

The contact and attachment opportunities between oil droplets and gas bubbles will be increased when the gas holdup increases (NETL 2017). As stated by Ran et al. (2013), higher gas holdup in the flotation system led to better oil separation efficiency. Xia et al. (2011) investigated gas holdup in a cyclone-static flotation column and found that gas holdup is higher in the top and central part of the column and is lower at the column bottom and in the areas near the column wall. Etchepare et al. (2017b) reported that the gas holdup is related to the operating pressure which dissolves air into the water in a pressure tank. In their experiments, when the operating pressure was in the range of 4 to 5 bars, the highest gas holdup value of 6.8% was achieved along with the highest concentration of NBs. Rollbusch et al. (2015) studied the relationship between gas holdup and pressure using nitrogen and DI water, and they found that gas holdup increased with the increase of pressure and noted that higher pressure caused increased bubble breakage which resulted in smaller bubbles. In terms of temperature effects, Pérez-Garibay et al. (2012) reported a reduction in gas holdup with a temperature increase from 10 to 30 °C.

2.5.3 Recycle ratio

In DGF system, the recycle ratio is the percentage of treated wastewater that is introduced back into the saturator vessel where it is pressurized and recycled to the flotation cell (Atarah, 2011). Fanaie et al. (2019) indicated that recycle ratio is a significant design parameter that will influence the gas concentration in the flotation system which directly impacts the overall performance of the treatment process. Li et al. (2007) stated that clarified effluent recycling can reduce the use of clean water in the saturator vessel and reduce the overall volume of chemical reagents added to the flotation process and their effectiveness. Wang et al. (2010) suggested that the design range of recycle ratio can vary from 10–60% while Atarah (2011) suggested that the typical recycle ratio is in the range of 15–50% for different wastewater treatment process. Li et al. (2007) concluded that the increase of recycle ratio leads to better oil separation efficiency of flotation for oily wastewater treatment and the recycle ratio should be controlled in the range of 20–30%.

2.5.4 Interfacial tension

IFT is a predominant factor that governs the system stability by controlling gas bubble and oil droplet attachment (Posocco et al., 2016; Saththasivam et al., 2016). As indicated by Moeini et al. (2014), IFT represents the surface free energy across the interface which has a force to hold the surface of two different phases (e.g., oil, water, or gas) together. In the process of separating oil from oil-water emulsion, it is necessary to lower IFT between oil and water phases to facilitate the coalescence of oil droplets to enhance oil separation efficiency.

2.5.5 Spreading coefficient

In the gaseous bubble flotation treatment process for separating oil from oil-water emulsion, the oil spreading coefficient can be expressed as (Rawlins and Ly, 2012):

$$S_o = \gamma_{wg} - \gamma_{ow} - \gamma_{og} \tag{2.10}$$

Where γ_{wg}, γ_{ow} and γ_{og} are water-gas, oil-water, and oil-gas IFT (N/m), respectively.

Spreading coefficient is an important factor regarding the contact of oil droplets with gas bubbles. As illustrated in Figure 2.13, when the IFT at the water-gas interface is stronger than the sum of the IFTs at the oil-water interface and oil-gas interface, the value of S_o will be positive and gas bubbles will be completely surrounded by oil droplets. Otherwise, when S_o is negative, oil droplets can only attach to gas bubbles at some contact points instead of forming continuous layers over bubbles which makes the adherence quite weak (Radzi, 2016). To ensure the successful rise of oil droplets to the wastewater surface, it is necessary to form a complete layer of oil droplets over bubbles. This makes the oil particles robust enough to resist the impact of drag and gravitational forces without breaking up in the course of rising (Radzuan et al., 2016). As a result, in order to achieve a successful and effective flotation process, a positive S_o is required. Increasing temperature and salinity will slightly increase the spreading coefficient because the IFT is consequently lowered (Rawlins and Ly, 2012; Moeini et al., 2014). The spreading coefficient can also be increased by using chemical surfactants that decrease the IFT at the oil-water interface (Kumar and Mandal, 2018). Yan et al. (2020) summarized that the spreading time (typically < 10 ms) of the oil droplets on the bubble surface is reversely proportional to the spreading coefficient and directly proportional to the oil viscosity.

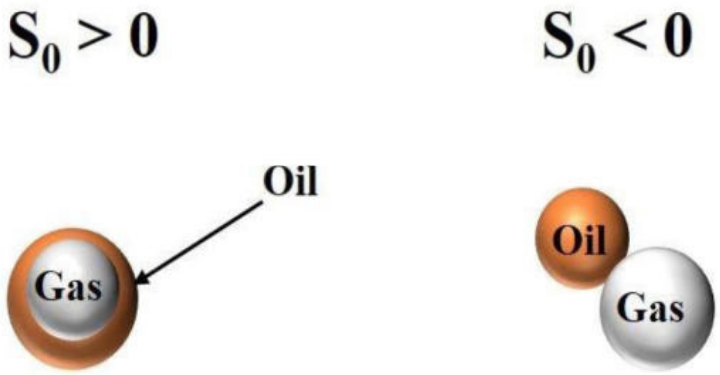

Figure 2.13 Schematic diagram of two different contact modes between oil droplet and gaseous bubbles (modified from Zhang et al., 2016)

2.6 Factors affecting oil separation efficiency in gas flotation

A variety of factors can affect the effectiveness of oil separation in gas flotation systems, and they include initial oil concentration in wastewater, oil droplet size, pH, temperature, gas pressure, salinity, and flotation time.

2.6.1 Initial oil concentration

Gas flotation is commonly used to treat oily wastewater with an initial oil concentration less than 1000 ppm (Saththasivam et al., 2016). When the oil concentration exceeds 1000 ppm, the efficiency of gas flotation could be reduced (Piccioli et al., 2020). Panneer Selvam (2018) observed a decreasing trend in oil separation efficiency from 92% to 72% when the initial oil concentration in wastewater was increased from 250 to 500 ppm. However, the majority of studies indicated that oil separation efficiency would increase with the increase of initial oil concentration. Van Le et al. (2013) treated finely emulsified palm oil using the combination of MBs and NBs flotation method and they achieved a 9% increase in oil separation efficiency after 30 min when they increased the initial oil concentration from 501 to 1009 ppm. Al-Dulaimi and Al-Yaqoobi (2021) used MB flotation column for oil-water separation in medium crude oil-water emulsion,

and they found improved oil separation efficiency from 46.29% to 73.12% after 165 min flotation when the initial oil concentration was increased from 200 to 300 ppm. As Alwared and Faraj (2015) stated, the increase of oil separation may be due to the enhancement of collision probability between gas bubbles and oil droplets in the emulsion.

2.6.2 pH

pH is an important factor for the emulsion breaking process (Figure 2.14). Using MB flotation to treat emulsified palm oil, Van Le et al. (2012) observed a substantial increase (more than 50%) in oil separation when the pH decreased from 8 to 3. Al-Dulaimi and Al-Yaqoobi (2021) enhanced oil separation efficiency by lowering the pH from alkaline to neutral and achieved the highest separation efficiency (75.19%) by further decreasing the pH to 3.32. Yasuda and Haneda (2015) used a MB generator to separate soybean oil from emulsion and they found that the oil separation efficiency increased with the decrease of pH. This effect was pronounced at pH levels below 4.5 where the oil separation ratio doubled when pH was reduced from 4 to 3. Acidifying emulsions with strong acid solutions such as H_2SO_4, HCl and HNO_3 before demulsification can be beneficial to the treatment process. According to Liu et al. (2021), oil droplets and gas bubbles usually have negative ZP in water. With a decrease in pH, the ZP of gas bubbles increases and reaches to zero when the pH is around 4.5, and further reducing the pH would result in positive ZP (Takahashi, 2005). As for oil droplets, the ZP also increases with a decreasing pH and gradually approaches zero (Yasuda and Haneda, 2015). Therefore, gas bubbles have a higher chance to attach to oil droplets due to the reduced repulsive force in a solution with a pH around 4.5. Especially when the pH is lower than 4.5, the positively charged gas bubbles can easily attach to negatively charged oil droplets because of the attractive force.

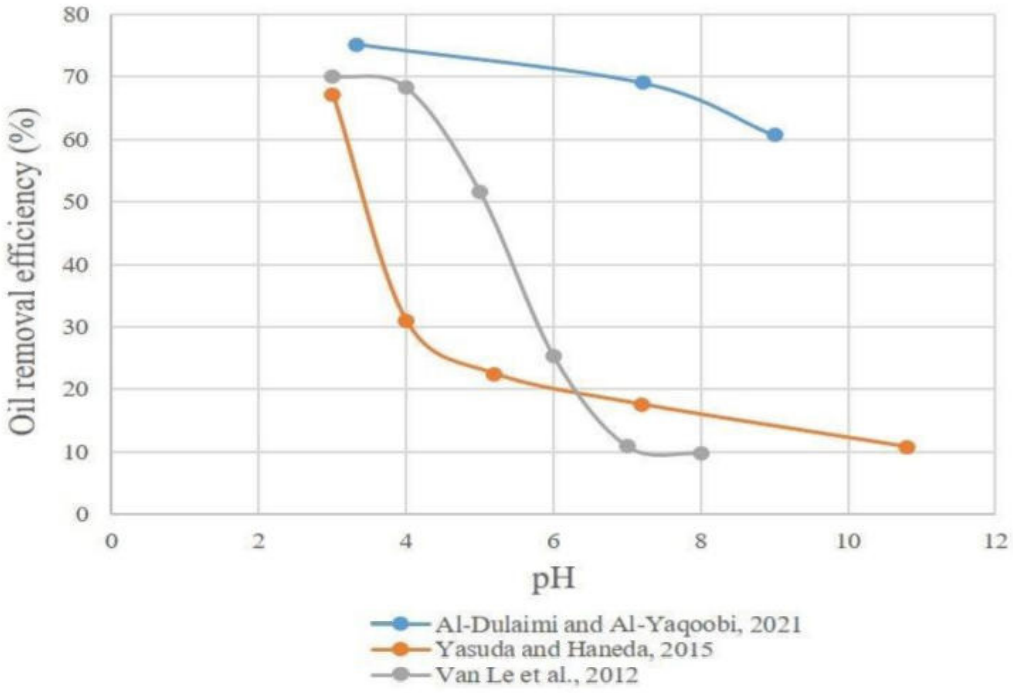

Figure 2.14 The effect of pH on oil separation efficiency using MBs gas flotation

2.6.3 Temperature

The effect of temperature on gas flotation has not been sufficiently studied yet. Qi et al. (2013) noticed an increase of oil separation from 83.4% to 92.2% when they raised the temperature from 12 °C to 40 °C, and they concluded that the increase in temperature led to decrease in elasticity and viscosity of the interfacial membrane. The decrease in elasticity and viscosity was due to the decrease in intermolecular cohesive forces under a relatively high temperature, which accelerated the coalescence of oil droplets. Radzuan et al. (2016) saw a slight increase in oil droplet separation efficiency of the experiments conducted at a higher temperature (35 °C) compared to that at room temperature for both vegetable oil and mineral oil. Jaji (2012) mentioned that when the temperatures exceeded 75 °C, the solubility of some hydrocarbons will be remarkably improved. Radzi (2016) noted that the viscosity of both the oil and water phase and surface

tensions were reduced at higher temperatures. Hasan et al. (2020) studied the effect of temperature on the viscosity of heavy crude oil, and they observed a reduction in viscosity from 10 Pa·s to 6.3 Pa·s when the temperature was increased from 25 °C to 75 °C. Furthermore, Bera et al. (2021) investigated the coalescence between oil droplets and observed higher coalescence frequencies at elevated temperatures (from 20 °C to 70°C). Sadeghi and Vissers (2020) used a laboratory scale flotation unit to investigate the effect of temperature on bubble size, and they found that the increase in temperature slightly reduced the size of large bubbles from 96 μm to 81 μm; however, it did not have significant effect on small bubbles (20 μm).

2.6.4 Pressure

DAF systems are usually designed and operated in the pressure range of 4–6 bar (Edzwald, 2010). According to Tetteh and Rathilal (2018), change of gas pressure that is utilized to dissolve gas in the water can affect the oil separation process. Larger gas bubbles will be produced when lower pressure is applied. The bubble size will affect flotation time which further influences the oil separation efficiency (Radzi, 2016). Etchepare et al. (2017a) noticed an increase of oil separation from 82% to 93% with the help of a flocculation polymer when the gas pressure increased from 2.5 to 3.5 bar, and when the pressure was further increased to 5 bar and 6 bar, the best results were achieved with separation efficiencies higher than 99%. In addition, they emphasized that DAF (pressure = 3.5 bar) can well meet the USEPA standard oil and grease emission level with a residual oil concentration of 28 ppm, which proved MBs and NBs-based gas flotation can work effectively at low pressure. Radzuan et al. (2016) increased the oil separation efficiency from 74.3% to 80.8% by increasing the pressure from 3 bar to 4 bar, and they indicated that when the gas pressure increased beyond 3.5 bar, the quantity of bubbles generated would

increase, but there was no significant change in the resulting bubble size. Zheng et al. (2015) investigated the performance of the DAF system under three different operational pressure (i.e., 2.5, 3, and 3.5 bar), and they increased the oil separation efficiency from 67.6% to 87.7%. Tetteh and Rathilal (2018) achieved improvement in oil separation efficiency with an increase in pressure from 2 bar to 5 bar, but when they further increased the pressure to 6 bar, a slight decrease in the efficiency was observed. As stated by Forero et al. (2007), even though the pressure can greatly assist the oil separation process, the extra energy consumption and operation cost caused by the increased pressure cannot be compensated by the increase in separation efficiency.

2.6.5 Salinity

Rajak et al. (2015) observed a significant increase in oil separation efficiency from 74.91% to 98.58% when the sodium chloride concentration was increased from 1wt% to 2wt%. Younker and Walsh (2014) investigated the oil separation performance by coagulation pre-treatment with ferric chloride and DAF process in both saline and fresh water. They found that the oil separation performance is better in saline water under different pH and coagulant doses, and this is because electrolytes in solution increase the ionic strength which correspondingly reduces the repulsive forces between oil droplets by double-layer compression. The addition of salt could decrease the mean diameter of gas bubbles due to the reduction in chances of bubble collision and coalescence, and the spreading coefficient could increase because of the decrease in oil-water IFT (Radzuan et al., 2016). As noted previously, the oil capture efficiency of gas bubbles increases with smaller bubbles (Balsley and Fitzpatrick, 2017). In addition, the dissolved oil concentration in the solution can be reduced by increasing the salinity of wastewater (Jaji, 2012).

2.6.6 Flotation time

Flotation time plays an important role in the oil separation efficiency of gas flotation systems (Figure 2.15). The increase in flotation time from 5 min to 25 min increased the oil separation efficiency from 69% (oil concentration = 154 ppm) to 82% (oil concentration = 92 ppm) when the initial oil concentration in the wastewater was 500 ppm (e Silva et al., 2018). Rajak et al. (2015) used air flotation to treat light crude oil emulsion with 20 g/L salinity and they observed that the oil recovery rate almost doubled when the flotation time increased from 10 min to 60 min. They concluded that the increase in flotation time results in the enhancement of attachment possibility between air bubble and oil droplets. Etchepare et al. (2017a) used isolated NBs with flocculation polymer (polyacrylamide) to treat oily wastewater with an inlet oil concentration of 334 ppm. They found that the oil separation efficiency increased by 27% with the increase of flotation time from 5 min to 10 min and further increase in flotation time had no significant effect on the separation efficiency. Al-Dulaimi and Al-Yaqoobi (2021) investigated the effect of flotation time on oil separation efficiency and found the separation increased by more than 60% when the flotation time increased from 30 to 240 min at initial oil concentration of 200 ppm. Van Le et al. (2012) increased the oil separation efficiency from 63% to 93% when they increased the flotation time from 2 min to 60 min with the help of a cationic surfactant (cetyltrimethylammonium chloride) at oil concentration of 1000 ppm.

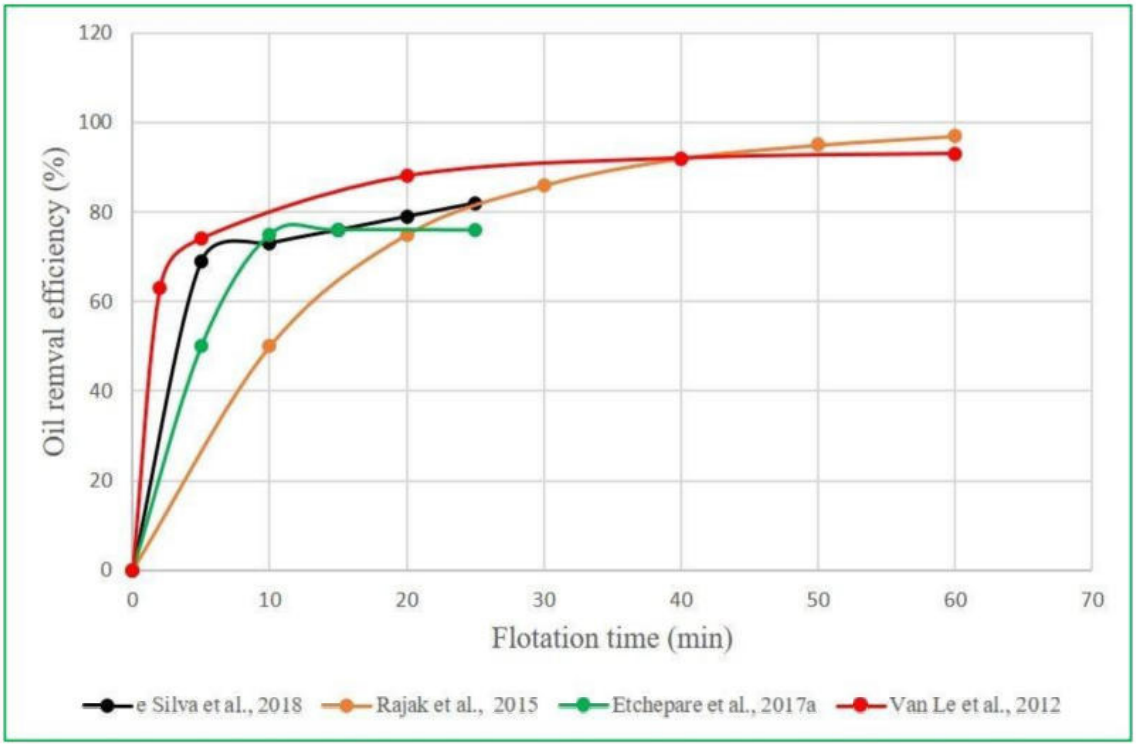

Figure 2.15 The effect of flotation time on oil separation efficiency

2.6.7 Oil droplet size

Gas flotation performs efficiently without adding chemicals when oil droplets have a diameter greater than 20 μm (Piccioli et al., 2020); however, it is not effective when the oil droplets are in dissolved form with a diameter less than 5 μm (da Silva et al., 2015). It has been reported that gas flotation is most effective when smallest possible gas bubbles are used to separate large oil droplets (Moosai and Dawe, 2003). Li et al. (2016a) used DAF to treat heavy crude oil emulsion and they observed a decrease in oil separation from 87.25% to 68.95% when the average oil droplet size decreased from 46.42 μm to 8.48 μm. Huang and Long (2020) found that the increase of oil droplet size from 22 μm to 41 μm led to an increase of oil separation efficiency by 7%. According to Santander et al. (2011), the efficiency of gas flotation is significantly related to the degree of emulsion destabilization. Demulsifiers are often used to destabilize water-oil emulsions to enlarge

the oil droplet size prior to the application of MBs and NBs based technologies (Zolfaghari et al., 2016). The oil droplet size enlargement can also be achieved by using some specific separators. For example, in the cyclonic separator, it is possible for oil droplets to coalesce due to speed difference inside the separator (Li et al., 2016a). Oil droplet size can be determined by a variety of procedures (Table 2.8).

Table 2.8 List of oil droplet size measurement methods

Methods	Reference
Mastersizer 2000 (Malvern, UK)	Kori et al., 2021
Zetasizer NanoZS laser diffractometer (Malvern, UK)	Salvia-Trujillo et al., 2013
Laser particle analyzer	Li et al., 2016a
Nuclear magnetic resonance spectrometer (Bruker, US)	Sommerling et al., 2016
Optical/Video microscopy + ImageJ software	Alade et al., 2021
AcoustoSizer II (Colloidal Dynamics LLC) instrument	Afuwape and Hill, 2021

2.7 Discussion and conclusions

Oil spills in the harsh, remote Arctic region would result in catastrophic consequences to the fragile Arctic ecosystem, and the risk of oil spills in this region is expected to increase as a result of the rapid climate change. It is important to develop effective and sustainable oil spill countermeasures to enhance the preparedness for oil spills in the Arctic. MBs and NBs-based gas flotation requires less energy consumption than some other wastewater treatment processes such as filtration and centrifugation. Furthermore, it will not generate significant direct GHG emissions or secondary pollution. Therefore, it is considered to be an environmentally friendly process that is effective for oil-water separation from emulsions. Due to their small bubble size, MBs and NBs

have wide surface area and rather slow rising velocity which help to better separate oil droplets from emulsions. The performance of MBs and NBs-based gas flotation treatment process is greatly affected by many factors, such as initial oil concentration, gas pressure, salinity, flotation time, addition of demulsifiers, and oil droplet size. A deep understanding of the inter-play of these potential controlling factors is critical to achieve the best oil-water separation results. The application of MBs and NBs in oily wastewater treatment is promising and the synergistic effect of gas flotation with other treatment technologies (e.g., membrane separation, sorption) needs further investigation. Future work is also needed in terms of the assessment of the environmental impact (e.g., emissions) of the application of MBs and NBs-based flotation technology. The impact assessment results would be helpful to the transition towards the sustainable oil spill response and low-impact oily wastewater treatment.

Chapter 3 Materials and Methods

3.1 Materials

Fresh CHCO was recovered from the Western Canada Sedimentary Basin (WCSB) and provided by Multi-Partner Oil Spill Research Initiative (MPRI). Table 3.1 lists the physiochemical properties of fresh and weathered CHCO. Sodium chloride (NaCl, ≥ 99.0%) and sodium hydroxide (NaOH, ≥ 97.0%) were purchased from Sigma-Aldrich. Tetrachloroethylene (≥ 99.0%, Sigma-Aldrich) was used for sample extraction. Silica gel (100-200 mesh, Sigma-Aldrich) activated at 215 °C for 24 h was used to clean up the extract. Anhydrous sodium sulfate (≥ 99.0%, Sigma-Aldrich) dried at 215 °C for 24 h was used to separate traces of water from the extract. Ultrapure water (UPW) generated from a water purification system (Milli-Q ® Advantage A10) was used for oily wastewater preparation.

Table 3.1 Physiochemical properties of fresh and weathered CHCO

Properties	Value		Units
	Fresh	Weathered	
API gravity	20.8	12.6	degrees (°)
Density (at 25 °C)	0.926	0.979	g/cm^3
Dynamic viscosity (at 25 °C)	160.9	10222.0	mPa·s
Water content	599	427	mg/L
Saturates	52.6	50.9	wt.%
Aromatics	10.7	9.8	wt.%
Resins	24.5	20.8	wt.%
Asphaltenes	12.2	17.0	wt.%

3.2 Oil weathering

The oil weathering process was conducted by placing 5 g fresh CHCO under a well-ventilated chemical fume hood at room temperature for six days (Hassanshahi et al., 2022). The cumulative mass loss due to evaporation of volatile hydrocarbons at different times was recorded and plotted in Figure 3.1. The cumulative mass loss reached 16% after three days, and further weathering had no significant effect on mass loss (less than 1% in a day). Thus, CHCO with 16% weathering was used in this research as weathered oil.

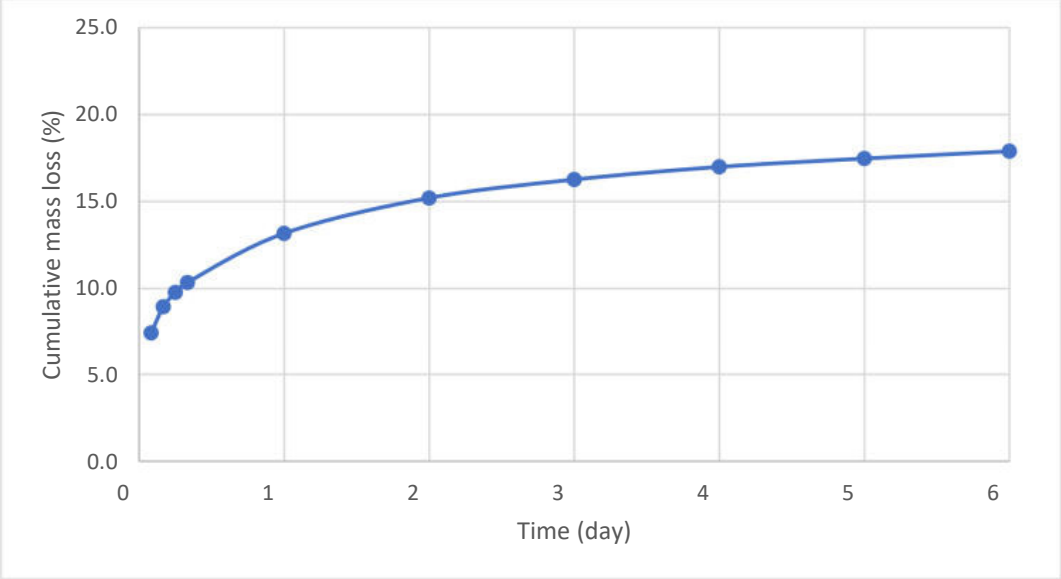

Figure 3.1 Cumulative mass loss of CHCO at different times

3.3 Preparation of oily wastewater

Artificial seawater was prepared by dissolving 35 g/L of NaCl in UPW to mimic the average salinity of real seawater (Lei et al., 2019). About 0.1 N sodium hydroxide (NaOH) solution was used to adjust the pH to 8.2, and a Mettler Toledo pH meter was used to measure the pH. Marine oily wastewater was prepared by dispersing the weighed amount of CHCO (fresh and weathered) in 2 L artificial seawater using an Ultra-Turrax homogenizer (IKA®, T50 model, 700

watts) equipped with a dispersing tool (IKA Works model: S50N-G45G). It was mixed at 5,000 rpm for 2 min and then at 10,000 rpm for 15 min. The homogenizer was turned off for 20 min after 10 min of operation to prevent the increase in the wastewater temperature. In this work, oily wastewater with initial oil concentrations of 200, 400, and 600 mg/L was prepared.

3.4 Experimental setup and procedure

All the experiments were carried out in a laboratory-scale gas flotation system (Fig. 2a). The cylindrical flotation column was made from clear polyvinyl chloride (PVC) with an internal diameter of 5.2 cm and a height of 100 cm. A fine bubble generator (LE5S, Living Energies & Co., Japan) capable of generating both MBs and NBs was used in this research, and its specifications are listed in Table 3.2. The existence of MBs can be seen from the milky appearance of the test water (Figure 3.2b). For each experiment, 2 L of oily wastewater was added to the flotation column from the top. Treated water was entirely recycled back to the bubble generator for bubble formation, and the bubble solution was introduced at the bottom of the column. After the flotation process, treated water samples were taken from sampling port 1 (Figure 3.2a) of the column for analysis. Control experiments were carried out in the same experimental setup (Figure 3.2a) without the generation of MBs and NBs.

Table 3.2 Summary of bubble generator specifications

Property	Value
Outer dimensions	H360mm × W310mm × D130mm
Weight	Approx. 4.4 kg
Electric power	AC 100-110V
Power frequency	50/60 Hz

Power consumption	1.3A
Capacity	200-300 cc/min
Temperature range	0 °C to 80 °C
Viscosity max.	50 mPas
Connecting tubing size	4mm (internal diameter) 6mm (external diameter)

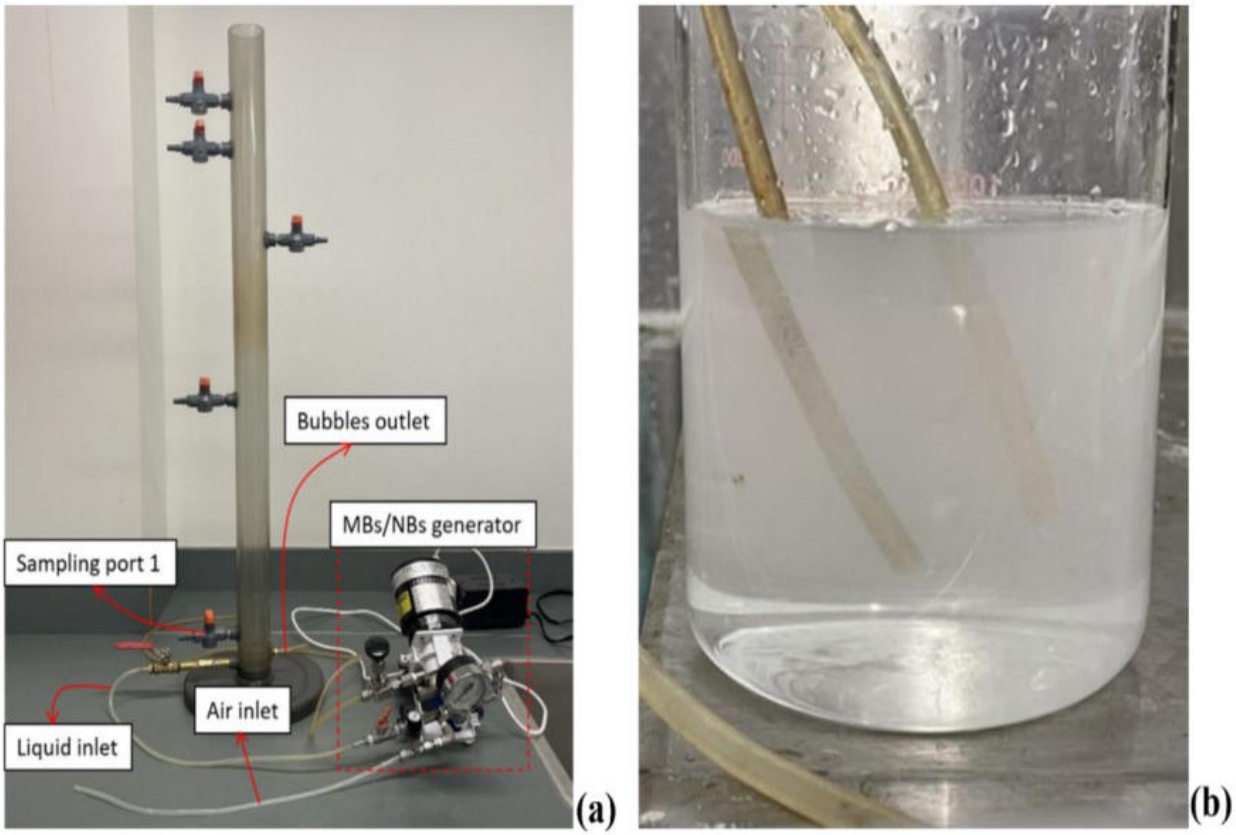

Figure 3.2 Laboratory MBs and NBs flotation setup (a) and appearance of MBs in test water (b)

3.5 Experimental design

Three experimental factors were investigated for their effects on oil separation efficiency, including initial oil concentration (X_1), flotation time (X_2), and temperature of inlet wastewater

(X_3). The selection of these factors and their levels was based on preliminary experiments, previous studies, and ambient environmental conditions. During the Deepwater Horizon oil spill, the average total petroleum hydrocarbon was 202 mg/L for all the seawater samples collected below the ocean surface (Sammarco et al., 2013). According to Saththasivam et al. (2016), gas flotation is commonly used to treat oily wastewater with an initial oil concentration of less than 1000 mg/L Therefore, an initial oil concentration range of 200–600 mg/L was selected in this study. A flotation time range of 10–30 min was selected based on the studies carried out by other researchers (Etchepare et al., 2017a; e Silva et al., 2018). The observation data of NASA's Aqua satellite indicated that the sea surface temperature ranges from -2 °C in polar regions to 35 °C in equatorial regions (Sea Surface Temperature, n.d.). Thus, a temperature range of 2–40 °C for inlet wastewater was selected.

RSM is an effective statistical tool for the optimization of different operational factors as well as for reducing the number of experimental runs (Wang et al., 2022a). A three-factor, three-level central composite design (CCD) was developed using RSM (Design Expert®, version 13.0). Table 3.3 lists the coded levels of different factors and their actual values. A total of 17 experimental runs with 3 replicates at the center point (to evaluate the pure error) were required. A detailed arrangement of experiments is shown in Table 3.4. The oil separation efficiency (Y) was selected as the response to evaluate the performance of the flotation process. The statistical significance of investigated variables and their interactions were determined by the analysis of variance (ANOVA). A quadratic polynomial equation used for predicting optimal conditions is expressed in Eq. (3.1).

$$Y = \beta_0 + \Sigma_{i=1}^{k}\beta_i x_i + \Sigma_{i=1}^{k}\beta_{ii} x_i^2 + \Sigma_{i=1}^{k-1}\Sigma_{i<j}^{k}\beta_{ij} x_i x_j \quad (3.1)$$

Where Y is the predicted response, k is the number of independent variables (k = 3 in this study), x_i and x_j are independent variables, β_0 is the constant coefficient, β_i is the linear effect, β_{ii} is the quadratic effect, and β_{ij} is the interaction effect between x_i and x_j (Hu et al., 2017; Zubair et al., 2022).

Confirmation experiments were performed at the optimum conditions to validate the mathematical model generated by RSM. The effect of crude oil conditions (fresh and weathered) was also investigated on the oil separation efficiency of the gas flotation system at the optimum conditions based on RSM results. In addition, single-factor experiments were also conducted to evaluate the influence of flotation time at wider levels on the oil separation efficiency. All the experiments were repeated three times, and their mean values were reported.

Table 3.3 Experimental range and levels of independent variables

Independent variables	Symbol	Coded levels			Units
		-1	0	+1	
Initial oil concentration	X_1	200	400	600	mg/L
Flotation time	X_2	10	20	30	min
Temperature of inlet wastewater	X_3	2	21	40	°C

Table 3.4 Experimental matrix of CCD design

Run	Initial oil concentration [a] (mg/L)	Flotation time [a] (min)	Temperature of inlet wastewater [a] (°C)
1	400 (0)	20 (0)	21 (0)
2	400 (0)	20 (0)	2 (-1)
3	400 (0)	30 (1)	21 (0)

4	200 (-1)	10 (-1)	2 (-1)
5	400 (0)	20 (0)	21 (0)
6	600 (1)	10 (-1)	2 (-1)
7	200 (-1)	30 (1)	40 (1)
8	200 (-1)	20 (0)	21 (0)
9	600 (1)	30 (1)	40 (1)
10	600 (1)	10 (-1)	40 (1)
11	400 (0)	20 (0)	40 (1)
12	400 (0)	10 (-1)	21 (0)
13	600 (1)	20 (0)	21 (0)
14	600 (1)	30 (1)	2 (-1)
15	200 (-1)	30 (1)	2 (-1)
16	400 (0)	20 (0)	21 (0)
17	200 (-1)	10 (-1)	40 (1)

[a] Values of coded levels (in parentheses) and actual values of experimental factors

3.6 Microscopy analysis

The morphology of oil droplets in the prepared wastewater was obtained through a compound microscope (Fisher Scientific AX800) with an objective magnification of 200 ×. The images were captured by a digital camera (Fisherbrand™ C-Mount Digital Camera) using SeBaView software (version 4.7) and were processed with ImageJ software to determine the oil droplet size and its distribution. For each sample, the diameters of at least 300 oil droplets were analyzed.

3.7 Oil concentration analysis

FTIR (Spectrum Two, PerkinElmer, USA) was employed to determine the oil concentration in the oily wastewater and the treated water by absorbance measurement (Farmaki et al., 2007). Tetrachloroethylene was used as an extraction solvent to extract oil from water samples due to its low toxicity (Sun et al., 2021). For each measurement, 20 mL of water sample was extracted following the standard ASTM D7066-04 (2017) method. The pure solvent was used as a blank. Infrared spectra were acquired at the wavelength range of 3200-2700 cm^{-1}. The oil separation efficiency was calculated based on the difference between the initial and the final oil concentration in the wastewater by Eq. (3.2):

$$Y = \frac{C_0 - C_r}{C_0} \times 100\% \quad (3.2)$$

Where Y is the oil separation efficiency (%), C_0 is the initial oil concentration (mg/L), and C_r is the residual oil concentration (mg/L) in the treated water.

Chapter 4 Results and Discussion

4.1 Size distribution of NBs

The sizes of NBs were measured using NanoSight NS500 (Malvern Instruments Ltd.), which uses nanoparticle tracking analysis (NTA) technology. As shown in Figure 4.1, the mean diameter and concentration of NBs were 102 nm and 4.27×10^8 particles/mL, respectively.

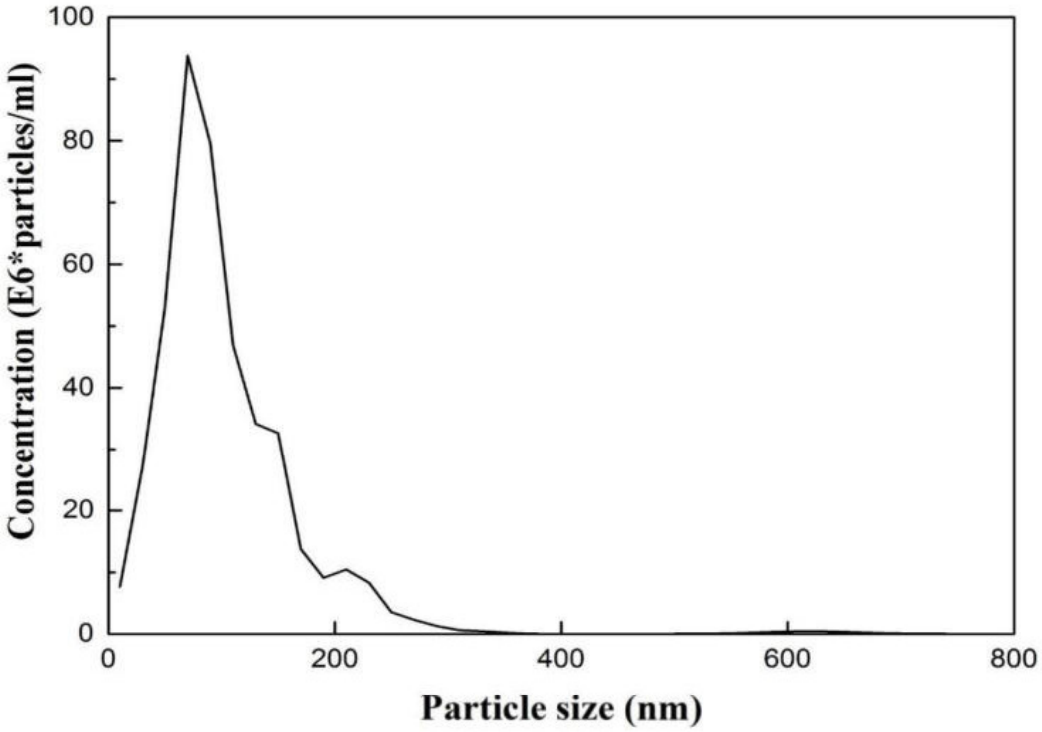

Figure 4.1 Particle size distribution of NBs

4.2 Regression model generation and statistical analysis

Table 4. 1 Results for oil separation efficiency of CHCO

Run	Oil separation efficiency (%)	
	Actual	Predicted
1	93.3	93.1

2	86.6	87.5
3	96.7	98.6
4	64.3	64.3
5	92.8	93.1
6	88.7	88.9
7	93.9	93.9
8	82.1	82.0
9	97.1	97.2
10	95.6	96.3
11	96.9	95.4
12	88.2	87.5
13	96.4	95.9
14	95.4	94.9
15	86.2	85.6
16	93.7	93.1
17	76.9	77.6

Table 4.2 ANOVA results of the regression model for oil separation efficiency

Source	Sum of Squares	df	Mean Square	F-value	p-value	
Model	1206.03	8	150.75	122.53	<0.0001	significant
X_1	487.20	1	487.20	395.98	<0.0001	
X_2	309.14	1	309.14	251.25	<0.0001	

X_3	153.66	1	153.66	124.89	<0.0001	
X_1X_2	117.81	1	117.81	95.75	<0.0001	
X_1X_3	17.11	1	17.11	13.91	0.0058	
X_2X_3	12.75	1	12.75	10.36	0.0123	
X_1^2	51.19	1	51.19	41.61	0.0002	
X_3^2	7.86	1	7.86	6.39	0.0354	
Residual	9.84	8	1.23			
Lack of Fit	9.44	6	1.57	7.73	0.1189	not significant
Pure Error	0.4067	2	0.2033			
Cor Total	1215.87	16				
Fit Statistics						
Std. Dev.	1.11		R^2	0.9919		
Mean	89.69		Adjusted R^2	0.9838		
C.V.%	1.24		Predicted R^2	0.9538		
			Adequate precision	42.5053		

The corresponding experimental results regarding oil separation efficiency based on CCD are shown in Table 4.1. It was found that the quadratic effect of X_2 was not significant for oil separation efficiency. Thus, this term was eliminated from the model. The following modified regression model for oil separation efficiency in the investigated experimental range was established:

$$Y = 23.86 + 0.16X_1 + 1.46X_2 + 0.68X_3 - 1.92 \times 10^{-3}X_1X_2 - 3.85 \times 10^{-4}X_1X_3 - 6.65 \times 10^{-3}X_2X_3 - 1.03 \times 10^{-4}{X_1}^2 - 4.46 \times 10^{-3}{X_3}^2 \quad (4.1)$$

Where Y is the oil separation efficiency (%), X_1, X_2, and X_3 represent initial oil concentration (200–600 mg/L), flotation time (10–30 min), and temperature of inlet wastewater (2–40 °C), respectively.

The significance of the model and the importance of the effect of each parameter were verified by ANOVA, and the associated results are shown in Table 4.2. A low p-value (<0.01%) and a high F-value (122.53) indicated that the generated model was significant and could well describe the oil separation efficiency. The lack of fit was insignificant, with a probability value of 0.1189 (>0.05), indicating that the developed model was suitably fitted to the experimental data and sufficiently accurate to predict the response. The coefficient of determination (R^2) reached 0.9919, while adjusted R^2 and predicted R^2 were 0.9838 and 0.9538, respectively. All the values of R^2 were high and very close to each other, which suggested a good fit of the regression model with high accordance between the experimental data and the predicted outcome. The signal-to-noise ratio (adequate precision) was desirable (>4), indicating the existence of sufficient signal and the capability of the generated model to predict results.

4.3 Effect of process parameters on oil separation efficiency

4.3.1 Effect of initial oil concentration

Based on ANOVA results, initial oil concentration was found to be the most critical factor in influencing the oil separation efficiency (F-value: 395.98, p-value < 0.0001). It is shown in Figure 4.2a that the increase of initial oil concentration in the oily wastewater could positively affect the oil separation efficiency. As listed in Table 3.4, increasing the initial oil concentration

from 200 mg/L to 600 mg/L greatly enhanced the oil separation efficiency by 14.3% (experimental runs #8 and #13), decreasing the effluent oil concentration from 36.8 mg/L to 23.7 mg/L. Generally, the increase in initial oil concentration led to a higher oil separation efficiency. However, a further increase in the oil concentration (> 500 mg/L) only brought a limited increase in oil separation efficiency. At higher oil concentrations, the oil droplets are denser and more uniformly distributed, which facilitates the bubble-oil aggregates to capture more oil droplets and therefore enhance the overall separation efficiency (Wang et al., 2022b; Shen et al., 2022).

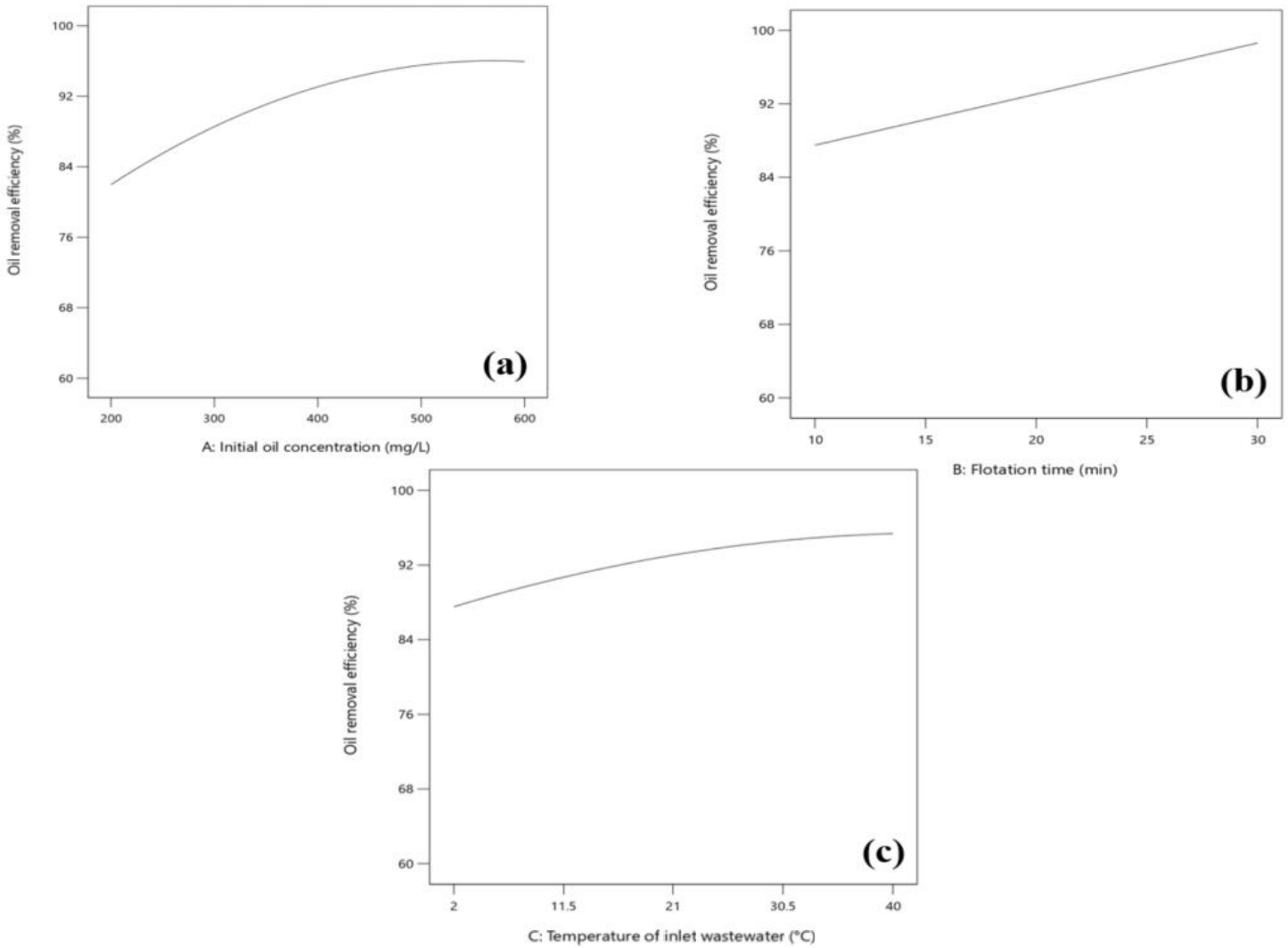

Figure 4.2 Predicted effects of experimental factors on oil separation efficiency, (a) flotation time: 20 min, temperature of inlet wastewater: 21 °C; (b) initial oil concentration: 400 mg/L, temperature of inlet wastewater: 21 °C; (c) initial oil concentration: 400 mg/L, flotation time: 20 min

4.3.2 Effect of flotation time

From Figure 4.2b, a trend can be observed in which oil separation efficiency increased with increasing flotation time in the experimental range of 10–30 min. A set of single-factor experiments were implemented to further investigate the effect of flotation time on oil separation efficiency, and the results are shown in Figure 4.3. Initial oil concentration and temperature of inlet wastewater were set at 400 mg/L and 21 °C, respectively. The oil separation efficiency was considerably enhanced in the first 15 min from 68.8% to 89.6%. The oil separation efficiency kept increasing with the increase in flotation time; however, the increasing rate was much slower after 15 min, especially after 40 min. At 60 min of flotation, it reached the highest oil separation efficiency of 98.7%. The positive effect of flotation time is mainly due to the increased encounters and interactions between gas bubbles and oil droplets at longer flotation times (Larsen, 2022). Although a longer duration of gas flotation helps to improve the oil separation performance, it is worth mentioning that controlling the flotation time under a certain limit is desirable for reducing the operational cost.

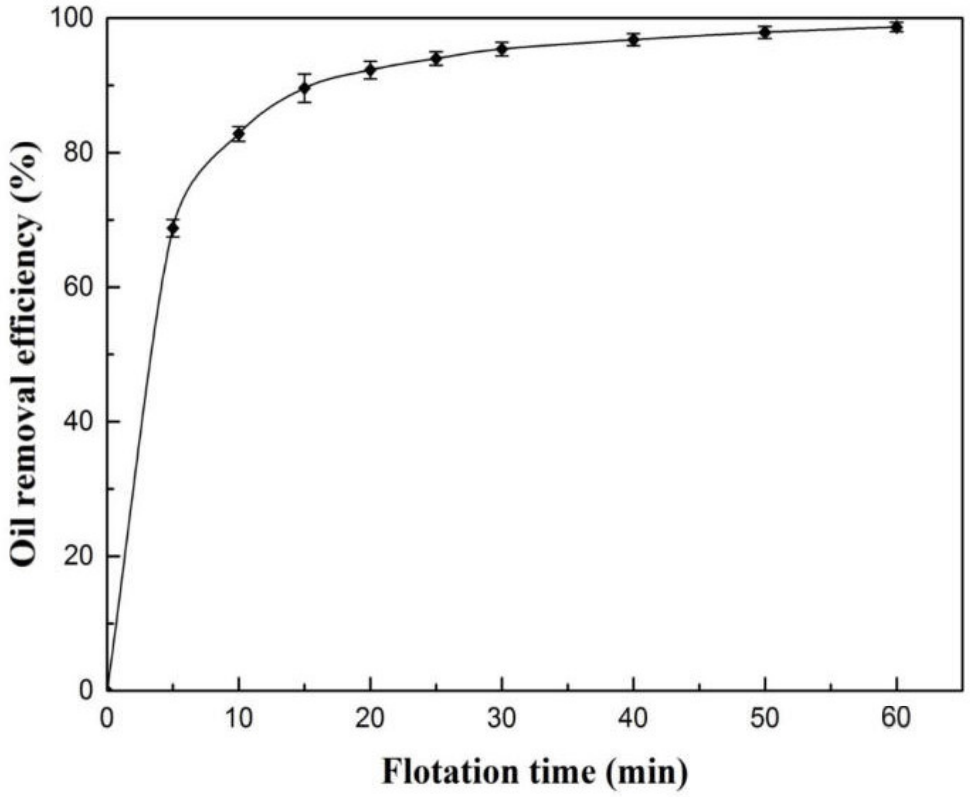

Figure 4.3 Effect of flotation time on oil separation efficiency

4.3.3 Effect of temperature of inlet wastewater

Temperature of inlet wastewater is also an essential factor that significantly affects the oil separation efficiency in the MBs and NBs gas flotation process. As shown in Figure 4.2c, by increasing the temperature of inlet wastewater, higher oil separation efficiencies were achieved. Results of the same experimental conditions indicated (experimental runs #2 and #11 in Table 3.4) that increasing the temperature of inlet wastewater from 2 °C to 40 °C led to an increase in oil separation efficiency from 86.6% to 96.9%. Correspondingly, the residual oil concentration in the treated water was reduced from 52.3 mg/L to less than 15 mg/L. There are several possible explanations for why the temperature of inlet wastewater might enhance oil separation with MBs and NBs gas flotation. First, as stated by Radzuan et al. (2016), the increasing temperature led to

a reduction in the viscosity of the fluids being treated, which increased the rising velocity of the oil droplets. Second, the increase in temperature may also enhance the coalescence frequency of oil droplets which will facilitate the oil separation (Piccioli et al., 2020).

4.3.4 Interaction of parameters

The interaction effects of experimental factors on the efficiency of MBs and NBs gas flotation were investigated. It can be found in Figure 4.4a that increasing flotation time resulted in enhanced oil separation efficiency at a low initial oil concentration, and this was attributed to adequate time for gas bubbles and oil droplets to attach and float to the liquid surface. Figure 4.4b shows the interactive reaction between the temperature of inlet wastewater and flotation time. When the temperature of inlet wastewater was high (e.g., 40 °C), a short flotation time (10 min) was sufficient to reach more than 90% of oil separation. A longer flotation time was needed to achieve similar results when the temperature of inlet wastewater was low. Furthermore, Figure 4.4c demonstrates the effect of changes in initial oil concentration and temperature of inlet wastewater on oil separation efficiency. As can be observed in the figure, the higher oil separation efficiency was obtained when both the initial oil concentration and temperature of inlet wastewater were kept at a higher value, which is consistent with the trends observed in Figure 4.4a and Figure 4.4c.

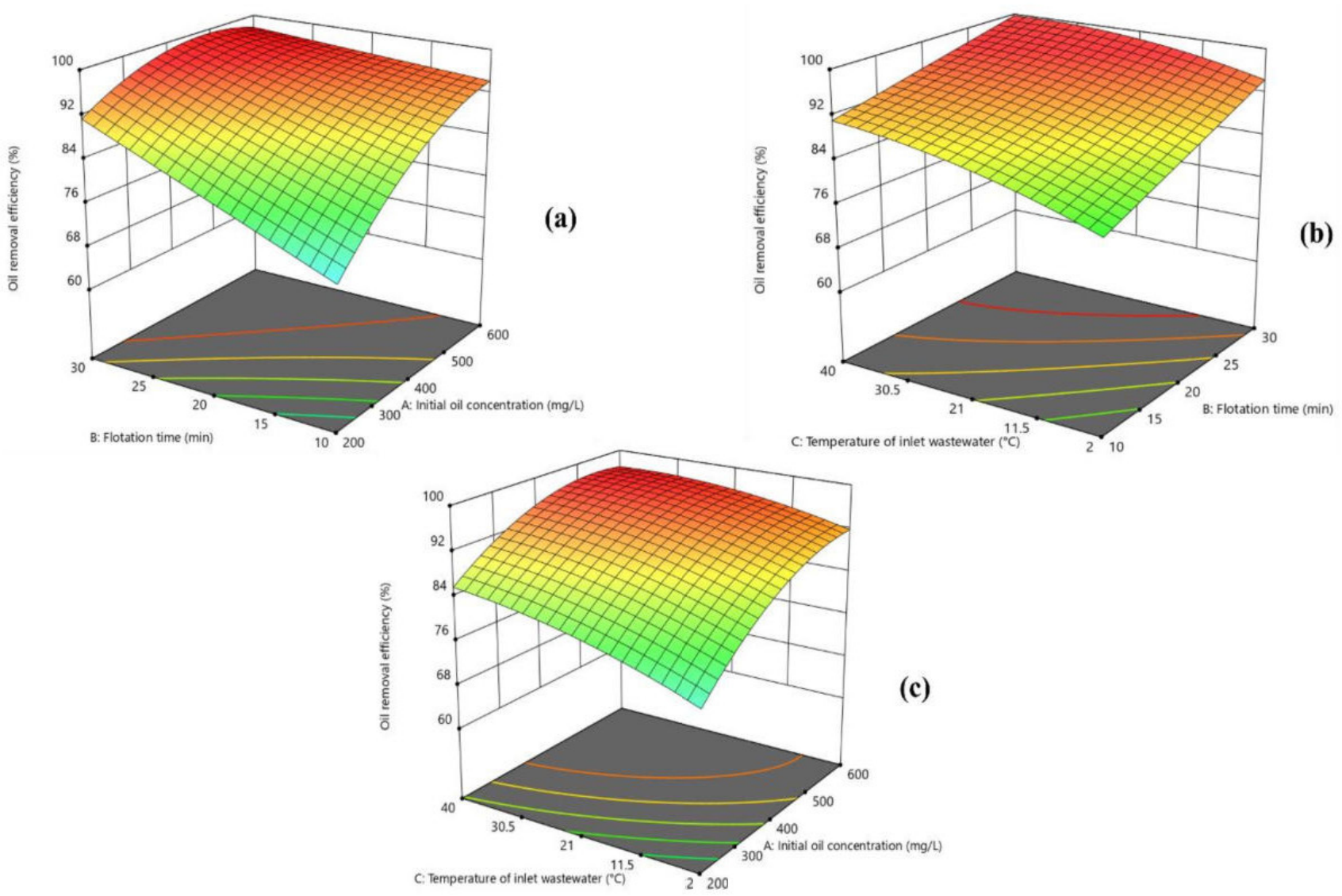

Figure 4.4 3D response surface graph showing the interaction effects of experimental factors on oil separation efficiency at (a) temperature of inlet wastewater = 21°C; (b) initial oil concentration = 400 mg/L; (c) flotation time = 20 min

4.4 Response surface optimization and validation of optimized results

In this study, the optimization of operational conditions for oil separation in gas flotation system was performed using Design Expert software version 13. To determine the optimum operational conditions, the oil separation efficiency was selected at the maximum value, and the target values of three independent variables were selected as in range. Based on the empirical model, the predicted maximum oil separation of 98.4% can be obtained at an initial oil concentration of 524.5 mg/L, flotation time of 28.6 min, and inlet wastewater temperature of 21.2°C. Under these conditions, the model's degree of desirability was equal to 1. To confirm the validity of the empirical model and the accuracy of the optimization results, three runs of confirmation experiments were conducted under the predicted optimal conditions. As shown in Table 4.3, an average oil separation efficiency of 97.3% was achieved with a standard deviation of 0.75 under the optimal conditions, which was in good agreement with the predicted value of 98.4%. Thus, it is evident that the obtained RSM model in this study can reasonably predict the oil separation efficiency by gas flotation system with MBs and NBs. All the experimental results from the confirmation experiments fell into the 95% prediction interval, further validating the model.

Table 4.3 Validation results with the actual and the predicted efficiency

Run	Actual efficiency (%)	Predicted efficiency (%)	Error (%)
1	97.4	98.4	-1
2	96.5	98.4	-1.9
3	98.0	98.4	-0.4
Mean efficiency	97.3	Standard deviation	0.75

4.5 Control experiments

Control experiments were designed to investigate the effect of the buoyant force of oil droplets in the prepared oily wastewater on oil separation efficiency. Three control experiments were conducted by leaving the prepared oily wastewater in the flotation column for gravity separation without flotation under the optimum experimental conditions obtained through RSM. In addition, the duration of gravity separation was extended from 28.6 min to 2 hours while the initial oil concentration and the temperature of inlet wastewater remained the same as the optimum values. It was observed from Figure 4.5 that after 28.6 min of gravity separation, the oil separation efficiency was 6.7%, and the oil separation efficiency reached 31.2% after 2 hours of gravity separation. However, after 28.6 min of gas flotation, the oil separation efficiency was greatly increased to 97.3%, which indicated that the application of MBs and NBs can significantly assist the separation of CHCO in the flotation system.

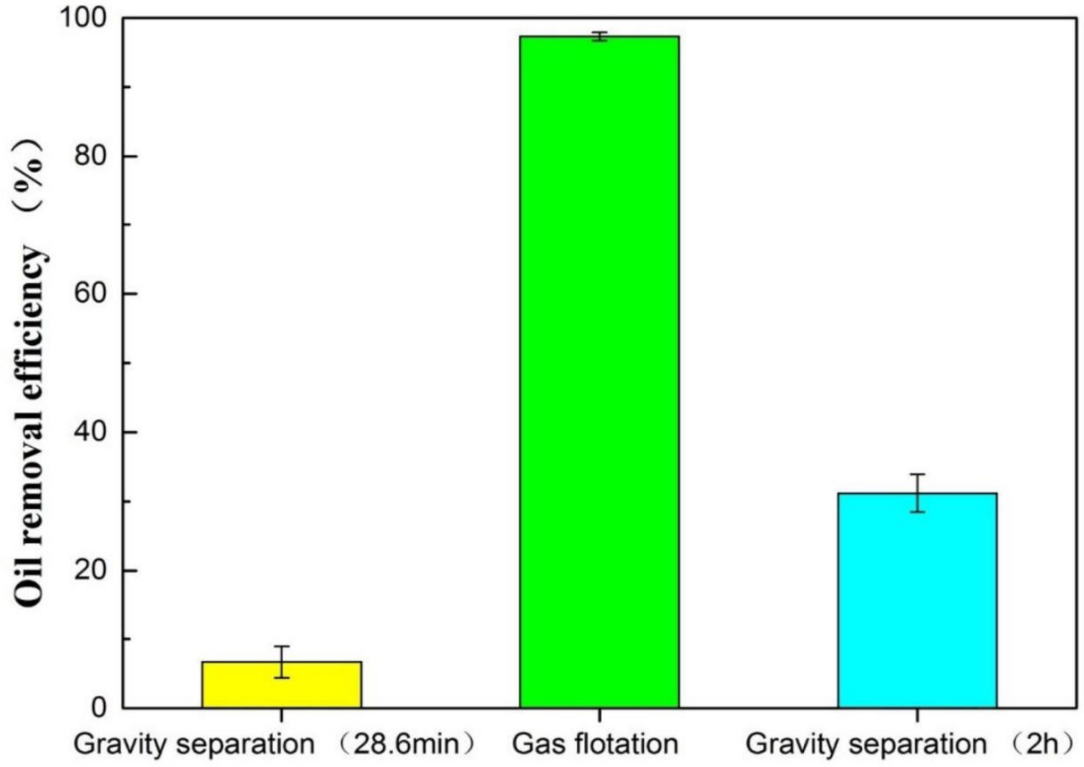

Figure 4.5 Comparison of oil separation efficiency between gravity separation and gas flotation

4.6 Effect of crude oil condition on oil separation efficiency

Both fresh and weathered oil were used to prepare oily wastewater. The generated wastewater was treated using MBs and NBs gas flotation under the optimum operational conditions obtained through RSM. The oil droplet size distribution in the oily wastewater generated by fresh and weathered CHCO was analyzed by ImageJ software. The microscopic images of the prepared oily wastewater and their corresponding oil droplet size distribution plots are shown in Figure 4.6. As presented in Figure 4.6, the average oil droplet size for the oily wastewater prepared with fresh and weathered CHCO were 24.51 μm and 29.29 μm, respectively.

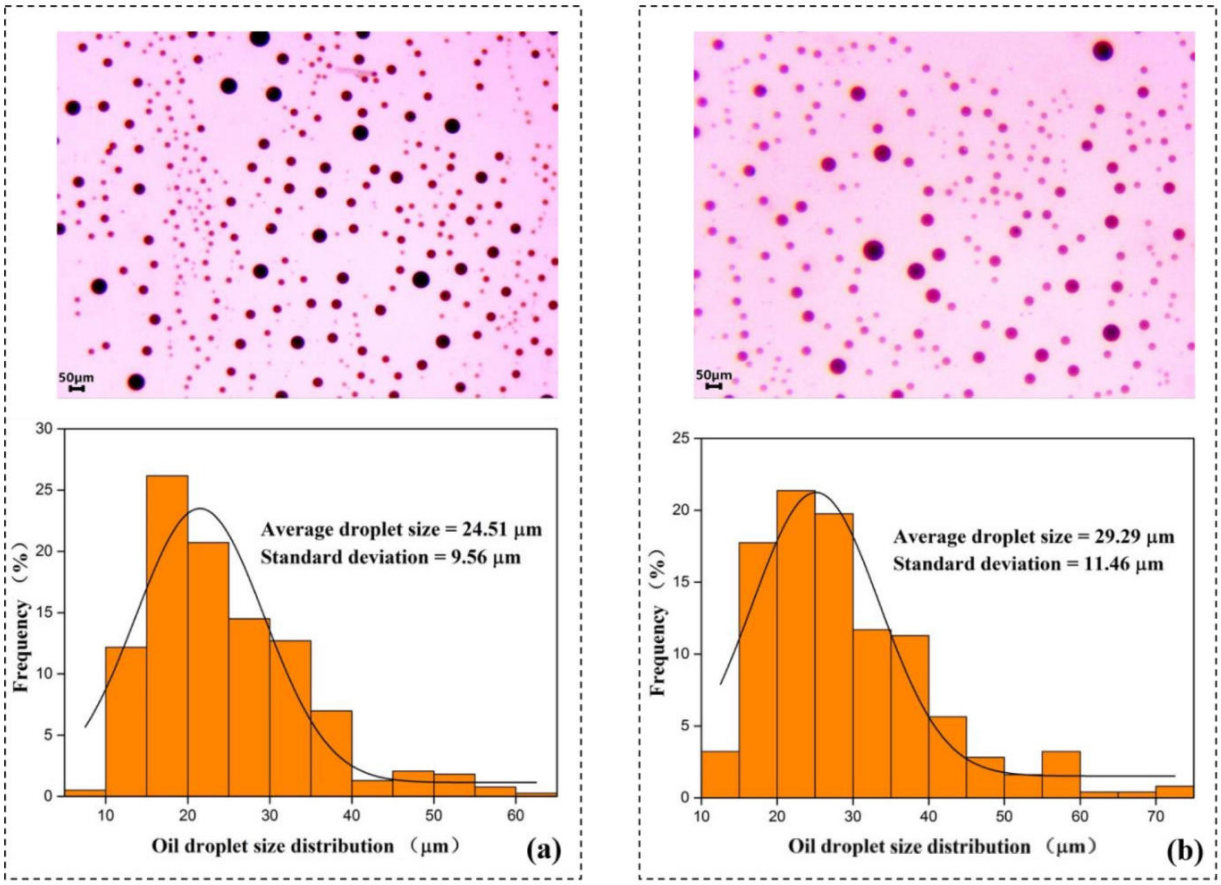

Figure 4.6 Microscopic images and corresponding oil droplet size distribution plots of the generated oily wastewater (a) with fresh CHCO, (b) with weathered CHCO

The effect of crude oil condition (fresh and weathered) on oil separation efficiency using MBs and NBs gas flotation was then studied, and the results are shown in Figure 4.7.

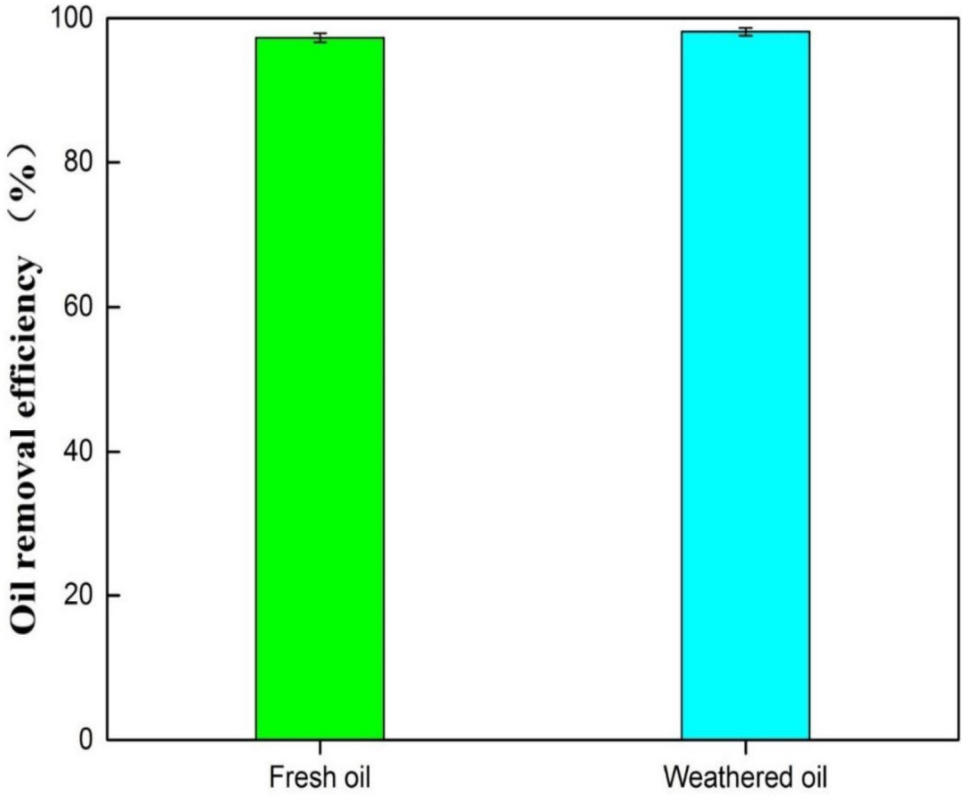

Figure 4.7 Effect of CHCO condition on oil separation efficiency

It can be seen from Figure 4.7 that there was no significant difference in oil separation efficiency between oily wastewaters containing fresh and weathered oil. After 28.6 min of gas flotation, the oil separation efficiency was 97.3% with fresh oil-contaminated oily wastewater. In comparison, the oil separation efficiency reached 98.2% for oily wastewater prepared with weathered oil after 28.6 min of gas flotation. Thus, it was suggested that gas flotation with MBs and NBs was effective at separating fresh as well as weathered crude oil.

Chapter 5 Conclusions

5.1 Research summary

In this study, the performance of MBs and NBs gas flotation in separating oil droplets from oily wastewater was investigated using RSM. Various initial oil concentrations, flotation times, and temperatures of inlet wastewater were examined to explore their effects on oil separation efficiency and the main findings of this paper are as follow:

(1) All three tested parameters were positively correlated with oil separation efficiency, and the influential effects were ranked as initial oil concentration (X_1) > flotation time (X_2) > temperature of inlet wastewater (X_3). A higher initial oil concentration could favor the oil separation process because of increased collision probability between oil droplets and gas bubbles. The oil separation was improved through the increase of flotation time; however, longer flotation time is not always desired considering the operational costs. The temperature of inlet wastewater also turned out to have a positive effect on the oil separation performance. Higher temperatures can reduce the viscosity of oil and water, which facilitates the rise and separation of oil from oily wastewater.

(2) The optimum treatment conditions are initial oil concentration of 524.5 mg/L, flotation time of 28.6 min, and inlet wastewater temperature of 21.2°C.

(3) In comparison to gravity separation, gas flotation remarkably improved oil separation. It can be observed that the oil separation efficiency increased by 90.6% with the presence of MBs and NBs when all the other conditions were kept the same.

(4) Oil separation efficiency was not affected by the crude oil condition. Thus, gas flotation with MBs and NBs can be used to treat both fresh and weathered oil spills.

(5) The use of MBs and NBs gas flotation appears to be an effective approach that not only helps significantly improve oil separation but also is chemical-free and scalable.

5.2 Limitations and future research

In this study, the laboratory-scale MBs and NBs gas flotation system was investigated to separate oil droplets from oily wastewater with high efficiency and easy operation. Although this method demonstrated promising results in the laboratory, its feasibility in large-scale application needs further verification. Due to limitations of time and lab resources, there are still some problems that need to be investigated and explored in depth. Recommendations for possible future research related to this study are listed as follows:

(1) Only one type of oil (heavy crude oil) was tested in this research. In the future, other types of oil including light and medium crude oil should also be investigated to compare if there is any difference in oil separation efficiency using MBs and NBs gas flotation.

(2) Air was used as the gas source in the current study. Different types of gas (e.g., nitrogen, ozone, and oxygen) should be used as the injection source in the future research.

(3) It is difficult to recover the separated oil (top layer) in the current flotation column. Once we took the treated water samples from the bottom of the column, the liquid level would drop and most of the separated oil would attach to the column wall. It is of great importance to design an oil skimming device that can recover the separated oil so that we can analyze the properties of the separated oil and possibly reuse the recovered oil afterwards.

(4) Future studies on the mechanisms of how NBs facilitate the flotation with MBs should be considered. The interaction between pollutant particles (oil droplets) with MBs and inter-pollutant particles when NBs can be observed should be focused in order to understand the reasons behind.

(5) When studying the effect of the temperature on oil separation, it is better to keep the ambient temperature the same as the wastewater temperature. In the current study, only the temperature of the oily wastewater going into the flotation column was controlled and the experiments were conducted under room temperature. So, during the course of the flotation experiments, the temperature of the wastewater definitely would gradually reach the room temperature.

References

Al-Maliky, S. B. (2010). Effect of geometrical dimensions and waste water temperature on the performance of an induced air flotation unit for the treatment of industrial waste water. Modern Applied Science, 4(6), 14-19.

Agarwal, A., Ng, W. J., & Liu, Y. (2011). Principle and applications of microbubble and nanobubble technology for water treatment. Chemosphere, 84(9), 1175-1180.

Atarah, J. J. A. (2011). The use of flotation technology in produced water treatment in the oil & gas industry (Master's thesis, University of Stavanger, Norway).

Ahmadi, R., & Khodadadi Darban, A. (2013). Modeling and optimization of nano-bubble generation process using response surface methodology. International journal of nanoscience and nanotechnology, 9(3), 151-162.

Arumugam, P. (2015). Understanding the fundamental mechanisms of a dynamic micro-bubble generator for water processing and cleaning applications. University of Toronto (Canada).

Alwared, A. I., & Faraj, N. S. (2015). Coagulation-flotation process for removing oil from wastewater using sawdust+ Bentonite. Journal of Engineering, 21(6), 62-76.

Alam, R. (2015). Fundamentals of electro-flotation and electrophoresis and applications in oil sand tailings management.

Azevedo, A., Etchepare, R., Calgaroto, S., & Rubio, J. (2016). Aqueous dispersions of nanobubbles: Generation, properties and features. Minerals Engineering, 94, 29-37.

Alheshibri, M., Qian, J., Jehannin, M., & Craig, V. S. (2016). A history of nanobubbles. Langmuir, 32(43), 11086-11100.

Attard, P. (2016). Pinning down the reasons for the size, shape, and stability of nanobubbles. Langmuir, 32(43), 11138-11146.

An, C., Huang, G., Yao, Y., & Zhao, S. (2017). Emerging usage of electrocoagulation technology for oil removal from wastewater: A review. Science of the Total Environment, 579, 537-556.

American Society of Testing and Materials (ASTM). (2017). ASTM D7066-04, Standard test method for dimer/trimer of chlorotrifluoroethylene (S-316) recoverable oil and grease and nonpolar material by infrared determination. West Conshohocken, PA.

Alam, H. S., Redhyka, G. G., Sugiarto, A. T., Salim, T. I., & Robbihi, I. (2018). Design and performance of swirl flow microbubble generator. International Journal of Engineering & Technology, 7(4), 66-69.

Ahmed, A. K. A., Sun, C., Hua, L., Zhang, Z., Zhang, Y., Zhang, W., & Marhaba, T. (2018). Generation of nanobubbles by ceramic membrane filters: The dependence of bubble size and zeta potential on surface coating, pore size and injected gas pressure. Chemosphere, 203, 327-335.

Afuwape, G., & Hill, R. J. (2021). Interfacial Dynamics of SDS-Stabilized Hexadecane-In-Water Nanoemulsions in the Megahertz Range. The Journal of Physical Chemistry C, 125(5), 3180-3191.

Alade, O. S., Mahmoud, M., Al Shehri, D. A., & Sultan, A. S. (2021). Rapid determination of emulsion stability using turbidity measurement incorporating artificial neural network (ANN): Experimental validation using video/optical microscopy and kinetic modeling. ACS omega, 6(8), 5910-5920.

Al-Dulaimi, S. L., & Al-Yaqoobi, A. M. (2021, February). Separation of oil/water emulsions by microbubble air flotation. In IOP Conference Series: Materials Science and Engineering (Vol. 1076, No. 1, p. 012030). IOP Publishing.

Bai, Z. S., Wang, H. L., & Tu, S. T. (2011). Oil–water separation using hydrocyclones enhanced by air bubbles. Chemical Engineering Research and Design, 89(1), 55-59.

Behin, J., & Bahrami, S. (2012). Modeling an industrial dissolved air flotation tank used for separating oil from wastewater. Chemical Engineering and Processing: Process Intensification, 59, 1-8.

Balsley, A., & Fitzpatrick, M. (2017). Mitigation of Oil in Water Column: Mitigation Prototype Tests. COAST GUARD NEW LONDON CT NEW LONDON.

Bui, T. T., Nguyen, D. C., & Han, M. (2019). Average size and zeta potential of nanobubbles in different reagent solutions. Journal of Nanoparticle Research, 21(8), 1-11.

Brasileiro, P. P. F., dos Santos, L. B., Chaprão, M. J., de Almeida, D. G., Roque, B. A. C., dos Santos, V. A., Sarubbo, L.A. & Benachour, M. (2020). Construction of a microbubble generation and measurement unit for use in flotation systems. Chemical Engineering Research and Design, 153, 212-219.

Bacosa, H. P., Kang, A., Lu, K., & Liu, Z. (2021). Initial oil concentration affects hydrocarbon biodegradation rates and bacterial community composition in seawater. Marine Pollution Bulletin, 162, 111867.

Bera, B., Khazal, R., & Schroën, K. (2021). Coalescence dynamics in oil-in-water emulsions at elevated temperatures. Scientific reports, 11(1), 1-10.

Badger S. (2019, September 19). Laser diffraction VS light scattering VS photo-optical analyzing. WS Tyler. https://blog.wstyler.com/cpa/laser-diffraction-vs-light-scattering-vs-photo-optical-analyzing

Calgaroto, S., Wilberg, K. Q., & Rubio, J. (2014). On the nanobubbles interfacial properties and future applications in flotation. Minerals Engineering, 60, 33-40.

Calgaroto, S., Azevedo, A., & Rubio, J. (2015). Flotation of quartz particles assisted by nanobubbles. International Journal of Mineral Processing, 137, 64-70.

Chandran, P., Bakshi, S., & Chatterjee, D. (2015). Study on the characteristics of hydrogen bubble formation and its transport during electrolysis of water. Chemical Engineering Science, 138, 99-109.

Campos, J. L., Valenzuela-Heredia, D., Pedrouso, A., Val del Río, A., Belmonte, M., & Mosquera-Corral, A. (2016). Greenhouse gases emissions from wastewater treatment plants: minimization, treatment, and prevention. Journal of Chemistry, 2016.

Cai, X., Chen, J., Liu, M., Ji, Y., Ding, G., & Zhang, L. (2017). CFD simulation of oil–water separation characteristics in a compact flotation unit by population balance modeling. Journal of Dispersion Science and Technology, 38(10), 1435-1447.

Crépin, A. S., Karcher, M., & Gascard, J. C. (2017). Arctic climate change, economy and society (ACCESS): Integrated perspectives. Ambio, 46(3), 341-354.

Chakibi, H., Hénaut, I., Salonen, A., Langevin, D., & Argillier, J. F. (2018). Role of bubble–drop interactions and salt addition in flotation performance. Energy & Fuels, 32(3), 4049-4056.

Chebbi, S., Allouche, A., Schwarz, M., Rabhi, S., Belkacemi, H., & Merabet, D. (2018). Treatment of produced water by induced air flotation: effect of both Tween 80 and ethanol concentrations on the recovery of PAHs. Nova Biotechnologica et Chimica, 17(2), 181-192.

Chawaloesphonsiya, N., Wongwailikhit, K., Bun, S., & Painmanakul, P. (2019). Stabilized Oily-Emulsion Separation Using Modified Induced Air Flotation (MIAF): Factor Analysis and Mathematical Modeling. Engineering Journal, 23(5), 29-42.

Chen, Z., An, C., Yin, J., Owens, E., Lee, K., Zhang, K., & Tian, X. (2021). Exploring the use of cellulose nanocrystal as surface-washing agent for oiled shoreline cleanup. Journal of Hazardous Materials, 402, 123464.

Dassey, A., & Theegala, C. (2011). Optimizing the air dissolution parameters in an unpacked dissolved air flotation system. Water, 4(1), 1-11.

da Silva, S. S., Chiavone-Filho, O., de Barros Neto, E. L., & Foletto, E. L. (2015). Oil removal from produced water by conjugation of flotation and photo-Fenton processes. Journal of environmental management, 147, 257-263.

da Cruz, S. G., Dutra, A. J., & Monte, M. B. (2016). The influence of some parameters on bubble average diameter in an electroflotation cell by laser diffraction method. Journal of environmental chemical engineering, 4(3), 3681-3687.

Desai, P. D., Ng, W. C., Hines, M. J., Riaz, Y., Tesar, V., & Zimmerman, W. B. (2019). Comparison of bubble size distributions inferred from acoustic, optical visualisation, and laser diffraction. Colloids and Interfaces, 3(4), 65.

Edzwald, J. K. (2010). Dissolved air flotation and me. Water research, 44(7), 2077-2106.

Eftekhardadkhah, M., Aanesen, S. V., Rabe, K., & Øye, G. (2015). Oil removal from produced water during laboratory-and pilot-scale gas flotation: The influence of interfacial adsorption and induction times. Energy & Fuels, 29(11), 7734-7740.

Eskin, A. A., Zakharov, G. A., Tkach, N. S., & Tsygankova, K. V. (2015). Intensification dissolved air flotation treatment of oil-containing wastewater. Modern Applied Science, 9(5), 114.

Etchepare, R., Oliveira, H., Azevedo, A., & Rubio, J. (2017a). Separation of emulsified crude oil in saline water by dissolved air flotation with micro and nanobubbles. Separation and Purification Technology, 186, 326-332.

Etchepare, R., Oliveira, H., Nicknig, M., Azevedo, A., & Rubio, J. (2017b). Nanobubbles: Generation using a multiphase pump, properties and features in flotation. Minerals Engineering, 112, 19-26.

e Silva, F. C. P. R., e Silva, N. M. P. R., da Silva, I. A., Brasileiro, P. P. F., Luna, J. M., Rufino, R. D., Santos, V.A. & Sarubbo, L. A. (2018). Oil removal efficiency forecast of a Dissolved Air Flotation (DAF) reduced scale prototype using the dimensionless number of Damköhler. Journal of Water Process Engineering, 23, 45-49.

Esmaeili, H., Mousavi, S. M., Hashemi, S. A., Lai, C. W., Chiang, W. H., & Bahrani, S. (2021). Application of biosurfactants in the removal of oil from emulsion. In Green Sustainable Process for Chemical and Environmental Engineering and Science (pp. 107-127). Elsevier.

Ebrahiem, E. E., Noaman, A. A., Mansour, M. I., & Almutairi, M. S. (2021). Produced Water Treatment Design Methods in the Gas Plant: Optimization and Controlling. Egyptian Journal of Chemistry, 64(7), 3597-3603.

Farmaki, E., Kaloudis, T., Dimitrou, K., Thanasoulias, N., Kousouris, L., & Tzoumerkas, F. (2007). Validation of a FT-IR method for the determination of oils and grease in water using tetrachloroethylene as the extraction solvent. Desalination, 210(1-3), 52-60.

Forero, J. E., Ortiz, O. P., & Duque[1], J. J. (2007). Design and application of flotation systems for the treatment of reinjected water in a colombian petroleum field. CT&F-Ciencia, Tecnología y Futuro, 3(3), 147-158.

Fonseca, R. R., Thompson Jr, J. P., Franco, I. C., & da Silva, F. V. (2017). Automation and control of a dissolved air flotation pilot plant. IFAC-PapersOnLine, 50(1), 3911-3916.

Fanaie, V. R., & Khiadani, M. (2020). Effect of salinity on air dissolution, size distribution of microbubbles, and hydrodynamics of a dissolved air flotation (DAF) system. Colloids and Surfaces A: Physicochemical and Engineering Aspects, 591, 124547.

Faghri, A., & Zhang, Y. (2020). Thermodynamics of multiphase systems. In Fundamentals of Multiphase Heat Transfer and Flow (pp. 39-93). Springer, Cham.

Favvas, E. P., Kyzas, G. Z., Efthimiadou, E. K., & Mitropoulos, A. C. (2021). Bulk nanobubbles, generation methods and potential applications. Current Opinion in Colloid & Interface Science, 54, 101455.

Farid, M. U., Choi, P. J., Kharraz, J. A., Lao, J. Y., St-Hilaire, S., Ruan, Y., Lam, P.K.S. & An, A. K. (2022). Hybrid nanobubble-forward osmosis system for aquaculture wastewater treatment and reuse. Chemical Engineering Journal, 435, 135164.

Gurung, A., Dahl, O., & Jansson, K. (2016). The fundamental phenomena of nanobubbles and their behavior in wastewater treatment technologies. Geosystem Engineering, 19(3), 133-142.

Genç, A., & Goc, S. (2018). Electroflotation of oily wastewater using stainless steel sponge electrodes. Water Science and Technology, 78(7), 1481-1488.

Gonzalez-Galvis, J. P., & Narbaitz, R. M. (2020). Large batch bench-scale dissolved air flotation system (LB-DAF) for drinking water treatability tests. Environmental Science: Water Research & Technology, 6(4), 1004-1017.

Hasan, S. W., Ghannam, M. T., & Esmail, N. (2010). Heavy crude oil viscosity reduction and rheology for pipeline transportation. Fuel, 89(5), 1095-1100.

Haarhoff, J., & Edzwald, J. K. (2013). Adapting dissolved air flotation for the clarification of seawater. Desalination, 311, 90-94.

Hassan, I., Nirdosh, I., & Sedahmed, G. H. (2015). Separation of oil from oil–water emulsions by electrocoagulation in an electrochemical reactor with a fixed-bed anode. Water, Air, & Soil Pollution, 226(8), 1-12.

Hoseini, S. M., Salarirad, M. M., & Alavi Moghaddam, M. R. (2015). TPH removal from oily wastewater by combined coagulation pretreatment and mechanically induced air flotation. Desalination and Water Treatment, 53(2), 300-308.

Hu, G., Li, J., Zhang, X., & Li, Y. (2017). Investigation of waste biomass co-pyrolysis with petroleum sludge using a response surface methodology. Journal of environmental management, 192, 234-242.

Huang, S., Ras, R. H., & Tian, X. (2018). Antifouling membranes for oily wastewater treatment: Interplay between wetting and membrane fouling. Current opinion in colloid & interface science, 36, 90-109.

Huang, J., Sun, L., Liu, H., Mo, Z., Tang, J., Xie, G., & Du, M. (2020). A review on bubble generation and transportation in Venturi-type bubble generators. Experimental and Computational Multiphase Flow, 2(3), 123-134.

Huang, Q., & Long, X. (2020). Analysis of the influencing factors on oil removal efficiency in large-scale flotation tanks: Experimental observation and numerical simulation. Energies, 13(4), 927.

Hassanshahi, N., Hu, G., & Li, J. (2022). Investigation of Dioctyl Sodium Sulfosuccinate in Demulsifying Crude Oil-in-Water Emulsions. ACS omega.

Issaka, S. A., Nour, A. H., & Yunus, R. M. (2015). Review on the fundamental aspects of petroleum oil emulsions and techniques of demulsification. Journal of Petroleum & Environmental Biotechnology, 6(2), 1.

Ismail, N. H., Salleh, W. N. W., Ismail, A. F., Hasbullah, H., Yusof, N., Aziz, F., & Jaafar, J. (2020). Hydrophilic polymer-based membrane for oily wastewater treatment: A review. Separation and Purification Technology, 233, 116007.

Jaji, K. T. (2012). Treatment of oilfield produced water with dissolved air flotation.

Jia, W., Ren, S., & Hu, B. (2013). Effect of water chemistry on zeta potential of air bubbles. Int. J. Electrochem. Sci, 8(4), 5828-5837.

Jamaly, S., Giwa, A., & Hasan, S. W. (2015). Recent improvements in oily wastewater treatment: Progress, challenges, and future opportunities. Journal of environmental sciences, 37, 15-30.

Kobayashi, D., Hayashida, Y., Sano, K., & Terasaka, K. (2011). Agglomeration and rapid ascent of microbubbles by ultrasonic irradiation. Ultrasonics sonochemistry, 18(5), 1193-1196.

Kumar, S., Kumar, R. A., Munshi, P., & Khanna, A. (2012). Gas hold-up in three phase co-current bubble columns. Procedia engineering, 42, 782-794.

Khirani, S., Kunwapanitchakul, P., Augier, F., Guigui, C., Guiraud, P., & Hébrard, G. (2012). Microbubble generation through porous membrane under aqueous or organic liquid shear flow. Industrial & engineering chemistry research, 51(4), 1997-2009.

Kyzas, G. Z., & Matis, K. A. (2016). Electroflotation process: A review. Journal of Molecular Liquids, 220, 657-664.

Kwak, D. H., & Chae, S. W. (2016). Solid thickening and methane production of livestock wastewater using dissolved carbon dioxide flotation. Water Quality Research Journal of Canada, 51(1), 17-25.

Kumar, S., Nandi, B. K., Guria, C., & Mandal, A. (2017). Oil removal from produced water by ultrafiltration using polysulfone membrane. Brazilian Journal of Chemical Engineering, 34, 583-596.

Kim, M. S., & Kwak, D. H. (2017). Effect of zeta potential on collision-attachment coefficient and removal efficiency for dissolved carbon dioxide flotation. Environmental engineering science, 34(4), 272-280.

Kumar, N., & Mandal, A. (2018). Surfactant stabilized oil-in-water nanoemulsion: stability, interfacial tension, and rheology study for enhanced oil recovery application. Energy & fuels, 32(6), 6452-6466.

Kyzas, G. Z., & Matis, K. A. (2018). Flotation in water and wastewater treatment. Processes, 6(8), 116.

Kang, W., Yin, X., Yang, H., Zhao, Y., Huang, Z., Hou, X., Sarsenbekuly, B., Zhu, Z., Wang, P., Zhang, X., Geng, J. & Aidarova, S. (2018). Demulsification performance, behavior and mechanism of different demulsifiers on the light crude oil emulsions. Colloids and Surfaces A: Physicochemical and Engineering Aspects, 545, 197-204.

Khalek, A., El Hosiny, F. I., Selim, K. A., & Osama, I. (2019). A novel continuous electroflotation cell design for industrial effluent treatment. Sustainable Water Resources Management, 5(2), 457-466.

Kim, M. S., Han, M., Kim, T. I., Lee, J. W., & Kwak, D. H. (2020). Effect of nanobubbles for improvement of water quality in freshwater: Flotation model simulation. Separation and Purification Technology, 241, 116731.

Kori, A. H., Mahesar, S. A., Sherazi, S. T. H., Khatri, U. A., Laghari, Z. H., & Panhwar, T. (2021). Effect of process parameters on emulsion stability and droplet size of pomegranate oil-in-water. Grasas y Aceites, 72(2), e410-e410.

Kyzas, G. Z., Mitropoulos, A. C., & Matis, K. A. (2021). From microbubbles to nanobubbles: effect on flotation. Processes, 9(8), 1287.

Kobayashi, T., Fujioka, S., Tanaka, S., & Terasaka, K. (2022). Microbubble generation with rapid dissolution of ammonia (NH3)-hydrogen (H2) mixed gas fed from a nozzle into water. Chemical Engineering Science, 248, 117155.

Lemos, R. C., da Silva, E. B., dos Santos, A., Guimaraes, R. C., Ferreira, B. M., Guarnieri, R. A., Dariva, C., Franceschi, E., Santos, A.F. & Fortuny, M. (2010). Demulsification of water-in-crude oil emulsions using ionic liquids and microwave irradiation. Energy & Fuels, 24(8), 4439-4444.

Li, X. B., Liu, J. T., Wang, Y. T., Wang, C. Y., & Zhou, X. H. (2007). Separation of oil from wastewater by column flotation. Journal of China University of Mining and Technology, 17(4), 546-577.

Liu, Z., Liu, J., Zhu, Q., & Wu, W. (2012). The weathering of oil after the Deepwater Horizon oil spill: insights from the chemical composition of the oil from the sea surface, salt marshes and sediments. Environmental research letters, 7(3), 035302.

Li, H., Hu, L., & Xia, Z. (2013). Impact of groundwater salinity on bioremediation enhanced by micro-nano bubbles. Materials, 6(9), 3676-3687.

Li, X., Xu, H., Liu, J., Zhang, J., Li, J., & Gui, Z. (2016a). Cyclonic state micro-bubble flotation column in oil-in-water emulsion separation. Separation and Purification Technology, 165, 101-106.

Li, X., Li, P., Zu, L., & Yang, C. (2016b). Gas-Liquid Mass Transfer Characteristics with Microbubble Aeration–I. Standard Stirred Tank. Chemical Engineering & Technology, 39(5), 945-952.

Li, P., Cai, Q., Lin, W., Chen, B., & Zhang, B. (2016c). Offshore oil spill response practices and emerging challenges. Marine pollution bulletin, 110(1), 6-27.

Liu, L., Yan, H., Zhao, G., & Zhuang, J. (2016). Experimental studies on the terminal velocity of air bubbles in water and glycerol aqueous solution. Experimental Thermal and Fluid Science, 78, 254-265.

Li, J., Song, Y., Yin, J., & Wang, D. (2017). Investigation on the effect of geometrical parameters on the performance of a venturi type bubble generator. Nuclear Engineering and Design, 325, 90-96.

Lucero Jr, A., Kim, D. S., & Park, Y. S. (2017). Parameter optimization for cost reduction of microbubble generation by electrolysis. Journal of Environmental Science International, 26(3), 269-280.

Lei, S., Zeng, M., Huang, D., Wang, L., Zhang, L., Xi, B., Ma, W., Chen, G. & Cheng, Z. (2019). Synergistic high-flux oil–saltwater separation and membrane desalination with carbon quantum dots functionalized membrane. ACS Sustainable Chemistry & Engineering, 7(16), 13708-13716.

Lee, J. I., Yim, B. S., & Kim, J. M. (2020). Effect of dissolved-gas concentration on bulk nanobubbles generation using ultrasonication. Scientific Reports, 10(1), 1-7.

Liang, H., & Esmaeili, H. (2021). Application of nanomaterials for demulsification of oily wastewater: A review study. Environmental Technology & Innovation, 22, 101498.

Larsen, R. A. G. (2022). Gas Flotation for Subsea Produced Water Treatment-Development of a Method (Master's thesis, NTNU).

Moosai, R., & Dawe, R. A. (2003). Gas attachment of oil droplets for gas flotation for oily wastewater cleanup. Separation and purification technology, 33(3), 303-314.

Matis, K. A., & Peleka, E. N. (2010). Alternative flotation techniques for wastewater treatment: focus on electroflotation. Separation Science and Technology, 45(16), 2465-2474.

Montes-Atenas, G., Garcia-Garcia, F. J., Mermillod-Blondin, R., & Montes, S. (2010). Effect of suspension chemistry onto voltage drop: Application to electro-flotation. Powder Technology, 204(1), 1-10.

Mohammed, A. A., & Al-Gurany, A. J. M. (2010). Separation of oil from O/W emulsion by electroflotation technique. Journal of Engineering, 3(16), 5503-5515.

Mohammed, T. J., Mohammed, S. S., & Khalaf, Z. (2013). Treatment of oily wastewater by induced air flotation. Eng. Technol. J, 31.

Moeini, F., Hemmati-Sarapardeh, A., Ghazanfari, M. H., Masihi, M., & Ayatollahi, S. (2014). Toward mechanistic understanding of heavy crude oil/brine interfacial tension: The roles of salinity, temperature and pressure. Fluid phase equilibria, 375, 191-200.

Maelum, M., & Rabe, K. (2015, March). Improving oil separation from produced water using new compact flotation unit design. In SPE Production and Operations Symposium. OnePetro.

Mishra, A. K., & Kumar, G. S. (2015). Weathering of oil spill: modeling and analysis. Aquatic Procedia, 4, 435-442.

Maeda, Y., Hosokawa, S., Baba, Y., Tomiyama, A., & Ito, Y. (2015). Generation mechanism of micro-bubbles in a pressurized dissolution method. Experimental Thermal and Fluid Science, 60, 201-207.

Meegoda, J. N., Aluthgun Hewage, S., & Batagoda, J. H. (2018). Stability of nanobubbles. Environmental Engineering Science, 35(11), 1216-1227.

Mohtashami, R., & Shang, J. Q. (2019). Electroflotation for treatment of industrial wastewaters: a focused review. Environmental processes, 6(2), 325-353.

Michailidi, E. D., Bomis, G., Varoutoglou, A., Kyzas, G. Z., Mitrikas, G., Mitropoulos, A. C., Efthimiadou, E.K. & Favvas, E. P. (2020). Bulk nanobubbles: Production and investigation of their formation/stability mechanism. Journal of colloid and interface science, 564, 371-380.

Mohammadiun, S., Hu, G., Gharahbagh, A. A., Li, J., Hewage, K., & Sadiq, R. (2021). Intelligent computational techniques in marine oil spill management: A critical review. Journal of Hazardous Materials, 419, 126425.

Naghdi, F. G., & Schenk, P. M. (2016). Dissolved air flotation and centrifugation as methods for oil recovery from ruptured microalgal cells. Bioresource technology, 218, 428-435.

Nordam, T., Dunnebier, D. A., Beegle-Krause, C. J., Reed, M., & Slagstad, D. (2017). Impact of climate change and seasonal trends on the fate of Arctic oil spills. Ambio, 46(3), 442-452.

Nordam, T., Beegle-Krause, C. J., Skancke, J., Nepstad, R., & Reed, M. (2019). Improving oil spill trajectory modelling in the Arctic. Marine pollution bulletin, 140, 65-74.

Norarat, R., Thonglek, V., & Ueda, Y. (2019). Size Distribution and Filtering Characteristics of Pressure Dissolved Oxygen Ultrafine Bubbles. aquaculture, 9, 11.

Nazari, S., & Hassanzadeh, A. (2020a). The effect of reagent type on generating bulk sub-micron (nano) bubbles and flotation kinetics of coarse-sized quartz particles. Powder Technology, 374, 160-171.

Nazari, S., Shafaei, S. Z., Hassanzadeh, A., Azizi, A., Gharabaghi, M., Ahmadi, R., & Shahbazi, B. (2020b). Study of effective parameters on generating submicron (nano)-bubbles using the hydrodynamic cavitation. Physicochemical Problems of Mineral Processing, 56.

Sea Surface Temperature (n.d.). NASA earth observatory. https://earthobservatory.nasa.gov/global-maps/MYD28M

Ohgaki, K., Khanh, N. Q., Joden, Y., Tsuji, A., & Nakagawa, T. (2010). Physicochemical approach to nanobubble solutions. Chemical Engineering Science, 65(3), 1296-1300.

Oh, S. H., Han, J. G., & Kim, J. M. (2015). Long-term stability of hydrogen nanobubble fuel. Fuel, 158, 399-404.

Oh, S. H., & Kim, J. M. (2017). Generation and stability of bulk nanobubbles. Langmuir, 33(15), 3818-3823.

Oliveira, H. A., Azevedo, A. C., Etchepare, R., & Rubio, J. (2017). Separation of emulsified crude oil in saline water by flotation with micro-and nanobubbles generated by a multiphase pump. Water Science and Technology, 76(10), 2710-2718.

Pendashteh, A. R., Abdullah, L. C., Fakhru'l-Razi, A., Madaeni, S. S., Abidin, Z. Z., & Biak, D. R. A. (2012). Evaluation of membrane bioreactor for hypersaline oily wastewater treatment. Process Safety and Environmental Protection, 90(1), 45-55.

Pérez-Garibay, R., Martínez-Ramos, E., & Rubio, J. (2012). Gas dispersion measurements in microbubble flotation systems. Minerals Engineering, 26, 34-40.

Parmar, R., & Majumder, S. K. (2013). Microbubble generation and microbubble-aided transport process intensification—A state-of-the-art report. Chemical Engineering and Processing: Process Intensification, 64, 79-97.

Posocco, P., Perazzo, A., Preziosi, V., Laurini, E., Pricl, S., & Guido, S. J. R. A. (2016). Interfacial tension of oil/water emulsions with mixed non-ionic surfactants: comparison between experiments and molecular simulations. RSC advances, 6(6), 4723-4729.

Palaniandy, P., Adlan, M. N., Aziz, H. A., Murshed, M. F., & Hung, Y. T. (2017). Dissolved air flotation (DAF) for wastewater treatment. In Handbook of advanced industrial and hazardous wastes management (pp. 657-694). CRC Press.

Panneer Selvam, A. K. (2018). Removal of dispersed oil drops by induced gas flotation (Master's thesis, NTNU).

Prakash, R., Majumder, S. K., & Singh, A. (2018). Flotation technique: Its mechanisms and design parameters. Chemical Engineering and Processing-Process Intensification, 127, 249-270.

Putatunda, S., Bhattacharya, S., Sen, D., & Bhattacharjee, C. (2019). A review on the application of different treatment processes for emulsified oily wastewater. International journal of environmental science and technology, 16(5), 2525-2536.

Piccioli, M., Aanesen, S. V., Zhao, H., Dudek, M., & Øye, G. (2020). Gas flotation of petroleum produced water: a review on status, fundamental aspects, and perspectives. Energy & Fuels, 34(12), 15579-15592.

Qi, W. K., Yu, Z. C., Liu, Y. Y., & Li, Y. Y. (2013). Removal of emulsion oil from oilfield ASP wastewater by internal circulation flotation and kinetic models. Chemical Engineering Science, 91, 122-129.

Rattanapan, C., Sawain, A., Suksaroj, T., & Suksaroj, C. (2011). Enhanced efficiency of dissolved air flotation for biodiesel wastewater treatment by acidification and coagulation processes. Desalination, 280(1-3), 370-377.

Rawlins, C. H., & Ly, C. (2012). Mechanisms for flotation of fine oil droplets. Separation Technologies for Minerals, Coal, and Earth Resources, 307.

Ran, J., Liu, J., Zhang, C., Wang, D., & Li, X. (2013). Experimental investigation and modeling of flotation column for treatment of oily wastewater. International Journal of Mining Science and Technology, 23(5), 665-668.

Rajak, V. K., Relish, K. K., Kumar, S., & Mandal, A. (2015). Mechanism and kinetics of separation of oil from oil-in-water emulsion by air flotation. Petroleum Science and Technology, 33(23-24), 1861-1868.

Rehman, F., Medley, G. J., Bandulasena, H., & Zimmerman, W. B. (2015). Fluidic oscillator-mediated microbubble generation to provide cost effective mass transfer and mixing efficiency to the wastewater treatment plants. Environmental research, 137, 32-39.

Rollbusch, P., Becker, M., Ludwig, M., Bieberle, A., Grünewald, M., Hampel, U., & Franke, R. (2015). Experimental investigation of the influence of column scale, gas density and liquid properties on gas holdup in bubble columns. International Journal of Multiphase Flow, 75, 88-106.

Radzuan, M. A., Belope, M. A. B., & Thorpe, R. B. (2016). Removal of fine oil droplets from oil-in-water mixtures by dissolved air flotation. Chemical Engineering Research and Design, 115, 19-33.

Radzi, A. R. M. (2016). Removal of oil droplets from oil-in-water mixtures by dissolved air flotation (DAF). University of Surrey (United Kingdom).

Rocha e Silva, F. C. P., Rocha e Silva, N. M. P., Luna, J. M., Rufino, R. D., Santos, V. A., & Sarubbo, L. A. (2018). Dissolved air flotation combined to biosurfactants: A clean and efficient alternative to treat industrial oily water. Reviews in Environmental Science and Bio/Technology, 17(4), 591-602.

Rosa, A. F., & Rubio, J. (2018). On the role of nanobubbles in particle–bubble adhesion for the flotation of quartz and apatitic minerals. Minerals Engineering, 127, 178-184.

Ross, V., Singh, A., & Pillay, K. (2019). Improved flotation of PGM tailings with a high-shear hydrodynamic cavitation device. Minerals Engineering, 137, 133-139.

Rameshkumar, C., Senthilkumar, G., Subalakshmi, R., & Gogoi, R. (2019). Generation and characterization of nanobubbles by ionization method for wastewater treatment. Desal Water Treat, 164, 98-101.

Santander, M., Rodrigues, R. T., & Rubio, J. (2011). Modified jet flotation in oil (petroleum) emulsion/water separations. Colloids and Surfaces A: Physicochemical and Engineering Aspects, 375(1-3), 237-244.

Sarkar, M. S. K. A. (2011). Electroflotation: Its application to water treatment and mineral processing (Doctoral dissertation, University of Newcastle).

Sammarco, P. W., Kolian, S. R., Warby, R. A., Bouldin, J. L., Subra, W. A., & Porter, S. A. (2013). Distribution and concentrations of petroleum hydrocarbons associated with the BP/Deepwater Horizon Oil Spill, Gulf of Mexico. Marine pollution bulletin, 73(1), 129-143.

Salvia-Trujillo, L., Rojas-Graü, M. A., Soliva-Fortuny, R., & Martín-Belloso, O. (2013). Effect of processing parameters on physicochemical characteristics of microfluidized lemongrass essential oil-alginate nanoemulsions. Food Hydrocolloids, 30(1), 401-407.

Shi, X., Tal, G., Hankins, N. P., & Gitis, V. (2014). Fouling and cleaning of ultrafiltration membranes: A review. Journal of Water Process Engineering, 1, 121-138.

Saththasivam, J., Loganathan, K., & Sarp, S. (2016). An overview of oil–water separation using gas flotation systems. Chemosphere, 144, 671-680.

Sommerling, J. H., Simon, A., Haber, A., Johns, M., Guthausen, G., & Nirschl, H. (2016). Interpretation of NMR diffusometry data regarding droplet size distributions in micro-and nanoemulsions. In XIII International Conference on the Applications of Magnetic Resonance in Food Science.

Shangguan, Y., Yu, S., Gong, C., Wang, Y., Yang, W., & Hou, L. A. (2018, March). A review of microbubble and its applications in ozonation. In IOP Conference Series: Earth and Environmental Science (Vol. 128, No. 1, p. 012149). IOP Publishing.

Sun, H., Liu, H., Wang, S., & Liu, Y. (2019). Remediation of oil spill-contaminated sands by chemical-free microbubbles generated in tap and saline water. Journal of hazardous materials, 366, 124-129.

Silva, E. J., Silva, I. A., Brasileiro, P. P., Correa, P. F., Almeida, D. G., Rufino, R. D., Luna, J.M., Santos, V.A. & Sarubbo, L. A. (2019). Treatment of oily effluent using a low-cost biosurfactant in a flotation system. Biodegradation, 30(4), 335-350.

Souza, J. S. B., Júnior, J. F., Simonelli, G., Souza, J. R., Góis, L. M. N., & Santos, L. C. L. (2020). Removal of oil contents and salinity from produced water using microemulsion. Journal of Water Process Engineering, 38, 101548.

Swart, B., Zhao, Y., Khaku, M., Che, E., Maltby, R., Chew, Y. J., & Wenk, J. (2020). In situ characterisation of size distribution and rise velocity of microbubbles by high-speed photography. Chemical Engineering Science, 225, 115836.

Sadeghi, F., & Vissers, A. J. (2020). Experimental Investigation of Bubble Size in Flotation: Effect of Salt, Coagulant, Temperature, and Organic Compound. SPE Production & Operations, 35(02), 384-392.

Sun, Y., Ma, J., Yue, G., Liu, S., Liu, H., Song, Q., & Wu, B. (2021). Comparisons of Four Methods for Measuring Total Petroleum Hydrocarbons and Short-term Weathering Effect in Soils Contaminated by Crude Oil and Fuel Oils. Water, Air, & Soil Pollution, 232(9), 1-14.

Shen, W., Mukherjee, D., Koirala, N., Hu, G., Lee, K., Zhao, M., & Li, J. (2022). Microbubble and nanobubble-based gas flotation for oily wastewater treatment: A review. Environmental Reviews, (ja).

Takahashi, M. (2005). ζ potential of microbubbles in aqueous solutions: electrical properties of the gas− water interface. The Journal of Physical Chemistry B, 109(46), 21858-21864.

Transports Canada. (2017, September 12). Environmental response systems: managing canada's marine oil spill preparedness and response regime. http://www.tc.gc.ca/eng/marinesafety/tp-tp14471-menu-1024.htm

Tansel, B., & Pascual, B. (2011). Removal of emulsified fuel oils from brackish and pond water by dissolved air flotation with and without polyelectrolyte use: Pilot-scale investigation for estuarine and near shore applications. Chemosphere, 85(7), 1182-1186.

Tsuge, H. (2014). Micro-and nanobubbles. Singapore: Pan Stanford.

Tamura, I., Uehara, I., & Adachi, K. (2014). Developing a micro-bubble generator and practical system for purifying contaminated water. Science and Technology Studies, 3(1), 87-90.

Temesgen, T., Bui, T. T., Han, M., Kim, T. I., & Park, H. (2017). Micro and nanobubble technologies as a new horizon for water-treatment techniques: A review. Advances in colloid and interface science, 246, 40-51.

Tetteh, E. K., & Rathilal, S. (2018, September). Investigating dissolved air flotation factors for oil refinery wastewater treatment. In CBU International Conference Proceedings (Vol. 6, pp. 1173-1177).

Tadesse, B., Albijanic, B., Makuei, F., & Browner, R. (2019). Recovery of fine and ultrafine mineral particles by electroflotation–A review. Mineral Processing and Extractive Metallurgy Review, 40(2), 108-122.

Ushikubo, F. Y., Enari, M., Furukawa, T., Nakagawa, R., Makino, Y., Kawagoe, Y., & Oshita, S. (2010a). Zeta-potential of micro-and/or nano-bubbles in water produced by some kinds of gases. IFAC Proceedings Volumes, 43(26), 283-288.

Ushikubo, F. Y., Furukawa, T., Nakagawa, R., Enari, M., Makino, Y., Kawagoe, Y., Shiina, T. & Oshita, S. (2010b). Evidence of the existence and the stability of nano-bubbles in water. Colloids and Surfaces A: Physicochemical and Engineering Aspects, 361(1-3), 31-37.

Ulatowski, K., Sobieszuk, P., Mróz, A., & Ciach, T. (2019). Stability of nanobubbles generated in water using porous membrane system. Chemical Engineering and Processing-Process Intensification, 136, 62-71.

Ulatowski, K., & Sobieszuk, P. (2020). Gas nanobubble dispersions as the important agent in environmental processes–generation methods review. Water and Environment Journal, 34, 772-790.

Ulatowski, K., Jeżak, R., & Sobieszuk, P. (2021). Impact of process parameters on the diameter of nanobubbles generated by electrolysis on platinum-coated titanium electrodes using Box–Behnken experimental design. Energies, 14(9), 2542.

Van Le, T., Imai, T., Higuchi, T., Doi, R., Teeka, J., Xiaofeng, S., & Teerakun, M. (2012). Separation of oil-in-water emulsions by microbubble treatment and the effect of adding coagulant or cationic surfactant on removal efficiency. Water science and Technology, 66(5), 1036-1043.

Van Le, T., Imai, T., Higuchi, T., Yamamoto, K., Sekine, M., Doi, R., Vo, H.T. & Wei, J. (2013). Performance of tiny microbubbles enhanced with "normal cyclone bubbles" in separation of fine oil-in-water emulsions. Chemical engineering science, 94, 1-6.

Wang, L. K., Shammas, N. K., Selke, W. A., & Aulenbach, D. B. (Eds.). (2010). Flotation technology (Vol. 12, p. 680). Totowa: Humana Press.

Wu, C., Nesset, K., Masliyah, J., & Xu, Z. (2012). Generation and characterization of submicron size bubbles. Advances in Colloid and Interface Science, 179, 123-132.

Wang, S., Liu, M., & Dong, Y. (2013). Understanding the stability of surface nanobubbles. Journal of Physics: Condensed Matter, 25(18), 184007.

Wilkinson, J., Beegle-Krause, C. J., Evers, K. U., Hughes, N., Lewis, A., Reed, M., & Wadhams, P. (2017). Oil spill response capabilities and technologies for ice-covered Arctic marine waters: A review of recent developments and established practices. Ambio, 46(3), 423-441.

Wiliński, P. R., Marcinowski, P. P., Naumczyk, J., & Bogacki, J. (2017). Pretreatment of cosmetic wastewater by dissolved ozone flotation (DOF). Desalination and Water Treatment, 71, 95-106.

Wu, W. (2017). Evaluation of a chemical dissolved air flotation system for the treatment of restaurant dishwasher effluents (Doctoral dissertation, The University of Regina (Canada)).

Wang, X., Shuai, Y., Zhou, X., Huang, Z., Yang, Y., Sun, J., Zhang, H., Wang, J. & Yang, Y. (2020). Performance comparison of swirl-venturi bubble generator and conventional venturi bubble generator. Chemical Engineering and Processing-Process Intensification, 154, 108022.

Wang, J. Y., Kadier, A., Hao, B., Li, H., & Ma, P. C. (2022a). Performance optimization of a batch scale electrocoagulation process using stainless steel mesh (304) cathode for the separation of oil-in-water emulsion. Chemical Engineering and Processing-Process Intensification, 174, 108901.

Wang, C., Lü, Y., Song, C., Zhang, D., Rong, F., & He, L. (2022b). Separation of emulsified crude oil from produced water by gas flotation: A review. Science of The Total Environment, 157304.

Wang, Y., Ma, H., Wang, X., Ju, L., Tian, L., Qi, H., Yu, H., He, G. & Li, J. (2022c). Study on the operation performance and floc adhesion mechanism of dissolved air flotation equipment. Environmental Science and Pollution Research, 1-15.

Xu, Q., Nakajima, M., Ichikawa, S., Nakamura, N., & Shiina, T. (2008). A comparative study of microbubble generation by mechanical agitation and sonication. Innovative food science & emerging technologies, 9(4), 489-494.

Xia, W., Yang, J., & Wang, Y. (2011). Reliability of gas holdup measurements using the differential pressure method in a cyclone-static micro-bubble flotation column. Mining Science and Technology (China), 21(6), 797-801.

Xia, Z., & Hu, L. (2016). Remediation of organics contaminated groundwater by ozone micro-nano bubble. Japanese Geotechnical Society Special Publication, 2(57), 1978-1981.

Xie, B. Q., Zhou, C. J., Sang, L., Ma, X. D., & Zhang, J. S. (2021). Preparation and characterization of microbubbles with a porous ceramic membrane. Chemical Engineering and Processing-Process Intensification, 159, 108213.

Younker, J. M., & Walsh, M. E. (2014). Impact of salinity on coagulation and dissolved air flotation treatment for oil and gas produced water. Water Quality Research Journal of Canada, 49(2), 135-143.

Yasuda, K., & Haneda, K. (2015). Separation of oil droplets from oil-in-water emulsion using a microbubble generator. Journal of Chemical Engineering of Japan, 48(3), 175-180.

Yau, Y. H., Rudolph, V., Ho, K. C., Lo, C. C. M., & Wu, K. C. (2017). Evaluation of different demulsifiers for Marpol oil waste recovery. Journal of water process engineering, 17, 40-49.

Yu, L., Han, M., & He, F. (2017). A review of treating oily wastewater. Arabian journal of chemistry, 10, S1913-S1922.

Yasuda, K., Matsushima, H., & Asakura, Y. (2019). Generation and reduction of bulk nanobubbles by ultrasonic irradiation. Chemical Engineering Science, 195, 455-461.

Yu, L., Kanezashi, M., Nagasawa, H., & Tsuru, T. (2020). Phase inversion/sintering-induced porous ceramic microsheet membranes for high-quality separation of oily wastewater. Journal of Membrane Science, 595, 117477.

Yan, S., Yang, X., Bai, Z., Xu, X., & Wang, H. (2020). Drop attachment behavior of oil droplet-gas bubble interactions during flotation. Chemical Engineering Science, 223, 115740.

Zasadowski, D., Strand, A., Sundberg, A., Edlund, H., & Norgren, M. (2014). Selective purification of bleached spruce TMP process water by induced air flotation (IAF). Holzforschung, 68(2), 157-165.

Zheng, T., Wang, Q., Shi, Z., Huang, P., Li, J., Zhang, J., & Wang, J. (2015). Separation of pollutants from oil-containing restaurant wastewater by novel microbubble air flotation and traditional dissolved air flotation. Separation Science and Technology, 50(16), 2568-2577.

Zolfaghari, R., Fakhru'l-Razi, A., Abdullah, L. C., Elnashaie, S. S., & Pendashteh, A. (2016). Demulsification techniques of water-in-oil and oil-in-water emulsions in petroleum industry. Separation and Purification Technology, 170, 377-407.

Zhang, Y., Shitta, A., Meredith, J. C., & Behrens, S. H. (2016). Bubble Meets Droplet: Particle-Assisted Reconfiguration of Wetting Morphologies in Colloidal Multiphase Systems. Small, 12(24), 3309-3319.

Zhao, L., Mo, Z., Sun, L., Xie, G., Liu, H., Du, M., & Tang, J. (2017). A visualized study of the motion of individual bubbles in a venturi-type bubble generator. Progress in Nuclear Energy, 97, 74-89.

Zhang, Y., Zhao, L., Deng, S., Zhao, R., Nie, X., & Liu, Y. (2019). Effect of nanobubble evolution on hydrate process: A review. Journal of Thermal Science, 28(5), 948-961.

Zhao, C., Zhou, J., Yan, Y., Yang, L., Xing, G., Li, H., Wu, P., Wang, M. & Zheng, H. (2021). Application of coagulation/flocculation in oily wastewater treatment: A review. Science of The Total Environment, 765, 142795.

Zubair, M., Aziz, H. A., Ihsanullah, I., Ahmad, M. A., & Al-Harthi, M. A. (2022). Enhanced removal of Eriochrome Black T from water using biochar/layered double hydroxide/chitosan hybrid composite: Performance evaluation and optimization using BBD-RSM approach. Environmental Research, 209, 112861.